DETECTION OF FÖRSTER CYCLE IN SINGLE

MOLECULES OF GREEN FLUORESCENT

PROTEIN

By

NATIS ZAD SHAFIQ

Bachelor of Science in Mechanical Engineering

Bangladesh University of Engineering & Technology

Dhaka, Bangladesh

2007

Submitted to the Faculty of the
Graduate College of the
Oklahoma State University
in partial fulfillment of
the requirements for
the Degree of
MASTER OF SCIENCE
July, 2011

DETECTION OF FÖRSTER CYCLE IN SINGLE

MOLECULES OF GREEN FLUORESCENT

PROTEIN

Thesis Approved:

Dr. Ali K. Kalkan

Thesis Adviser

Dr. David A. Rubenstein

Dr. Kevin D. Ausman

Dr. Mark E. Payton

Dean of the Graduate College

ACKNOWLEDGMENTS

This thesis work would not have been possible without the helpful suggestion and guidance provided by some individuals in one way or another. I am really grateful to those people whose honest perseverance soothed me in hard times. Their contribution proved to be invaluable in completing this work.

First and foremost, I want to extend my utmost gratitude to Dr. A.K. Kalkan. He is not only an adviser to me but also a philosophical friend of mine and to a great extent my mentor, too. He endured my shortcomings patiently and helped me to evolve as a sharper and more intuitive researcher. This thesis would not have been possible without his contribution. I would also like to thank my committee member, Dr. David Rubenstein and Dr. Kevin Ausman for lending their valuable time and feedback on this thesis. I am thankful to Dr. K. J. Hellingwerf for providing us with the GFP sample.

I would also like to extend my heartfelt gratitude to my friends at the Functional Nanomaterials Lab. Specially, my former colleague Kushagra Singhal, who helped me to get familiar with the Raman and UV-Vis spectrometers. He also shared his research experience with me and it proved to be very helpful. My other colleague and friend, Md. Shafayet Khurshid, also helped me in my research and together we learnt and shared a lot of ideas. I also want to thank my lab mate Çagri Özge Topal for helping me in my SM-SERS studies with helpful ideas.

All of my friends have been very supportive throughout my studies. Their support and patience helped me to keep myself calm in difficult times. I am especially grateful to my parents, my brother and my fiancé for their all through moral support.

TABLE OF CONTENTS

LIST OF TABLES

LIST OF FIGURES

CHAPTER I

INTRODUCTION

Green fluorescent protein (GFP), responsible for the interesting bioluminescence of the jellyfish *Aequorea victoria* found in the Northeastern Pacific, has gained an unequivocal recognition from being an esoteric protein to a widely utilized bio-imaging tool by revolutionizing the visualization of dynamic events inside a cell [1, 2]. The main reason behind such popularity of GFP like proteins came due to their ability to form a very stable chromophore without requiring any external cofactors [1]. In addition, extensive mutagenesis provided improved mutants of wild type GFP (wtGFP) with broadened spectral range from blue through cyan and green to yellow [2]. In 2008 due its indispensible role as a major tool in biotechnology GFP earned Nobel Prize in chemistry. As an extraordinary example of such immense impact of GFP mutants on bio-imaging, researchers from Harvard Brain Center have recently demonstrated a unique genetic strategy termed "Brainbow" to generate a vastly multicolored map of the neural circuits of brain by coloring individual neurons with a random mixture of green, cyan and yellow derivatives of GFP [3]. Although most innovations are still thriving in bio-imaging but interestingly enough a very recent demonstration of a single eGFP expressing kidney cell as the first living laser indicates the extent of versatility that remains to be explored [4]. Fluorescent protein technology in now rapidly harvesting a wide variety of applications by using a vast array

of GFP like proteins and thus the complete potential of these fluorescent proteins are becoming fully realized.

GFP has a highly fluorescent chromophore embedded inside its unique β-barrel structure [1, 5, 6]. The high quantum yield (0.8) of GFP is associated with a tightly shielded chromophore located centrally inside the folded β-sheets and adopts a cis and nearly planar configuration upon folding [1, 5-7]. It is understood that the folded protein structure is important for the fluorescence of GFP chromophore, as the isolated chromophore is found to be non-fluorescent [1, 8]. It is well established that wtGFP is found as deprotonated-cis (B-state) and protonated-cis (A-state) forms of the chromophore and interconversion between these two states rarely occurs [1]. The wtGFP population is present in a 6:1 ratio of A-to-B forms in thermodynamic equilibrium at room temperature and pH=7, but prolonged and intense UV excitation of the A-form can promote the conversion to B-form on a longer timescale [1]. GFP became an interesting subject due to its unique spectroscopic properties, one of which includes the emission of green fluorescence irrespective of exciting either of the two dominant forms [1]. This important feature of wtGFP eventually led to the discovery that photoexcited chromophore acts as a photoacid and triggers an ultrafast excited state proton transfer (ESPT) reaction [1, 9]. Although such excited protolytic reaction (i.e. "Förster cycle") is well established in simple chemical systems, this discovery proved to be unique in biological systems [9]. A seminal work by Chattoraj *et al.* on the scheme of interconverting states of wtGFP proposed an excited state proton transfer mechanism via an excited anion of an intermediate ground state (I) [10, 11]. The "Förster cycle" is promoted by exciting the A-form under UV light by generating an excited form of A-state (A*)-state which quickly converts (on a timescale of picosecond) to an excited intermediate anion (I*) upon proton transfer [10]. This excited I* -state relaxes back to the ground intermediate state (I) by giving similar green fluorescence as emitted by the excited B-state [10, 11]. Eventual reprotonation of I-state populates the ground A-state [10, 11]. In this specific protolytic reaction, the B-form of the

chromophore can be populated with a low probability by reorganization of the surrounding protein structure about I*-state [10]. Recent study using spectral hole burning at 1.6 K distinctively identified these two anionic species: I and B, in addition to the dominant A-form [12]. These high resolution hole burning experiments confirmed the proposed radiative interconversion pathway: A→A*→I*→I →A (i.e. "Förster cycle"), in addition to the rare radiationless interconversion: I*→B*→B [12].
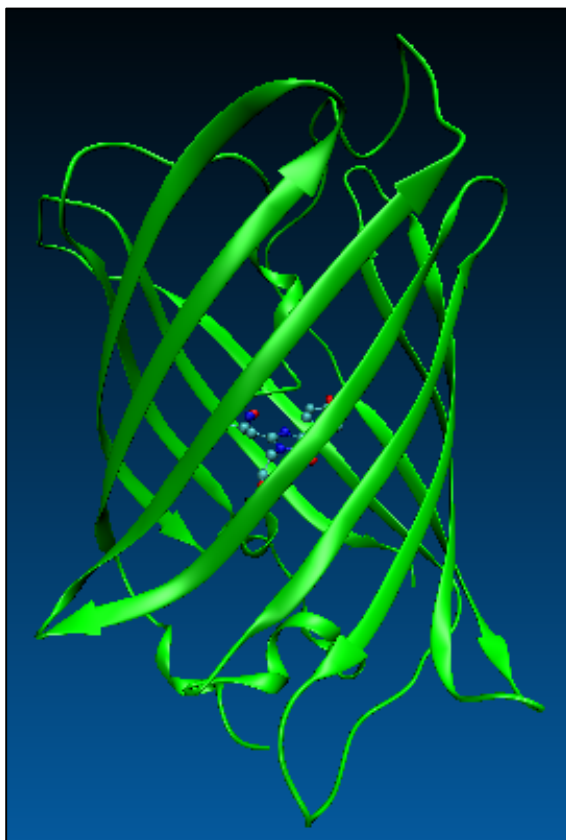
Figure I.1. Three dimensional structure of wtGFP showing the tertiary β-fold with centrally located *p*-hydroxybenzylideneimidazolinone chromophore, Protein Data Bank accession number 1EMA [1, 5].

Although vibrational spectroscopy has been employed to understand such light induced characteristics of GFP, but the extent remained limited in establishing a relationship between the excited state proton acceptor (Glu222) and the overall rate of ESPT beside assigning dominant vibrational modes of the chromophore [13, 14] . The results of these vibrational studies (infrared

absorption, Raman, resonance Raman) are mostly employed on the isolated model chromophore of GFP without taking into account the surrounding protein environment [15-19]. But substantial dynamic differences are present during ESPT between the isolated model compound and GFP, as green fluorescence is essentially lost for theses model chromophores [2]. Assignments of these vibrational modes are done by comparing experimental results with the theoretical calculations based on the isolated neutral, cationic or anionic forms of the model chromophore [15-17, 19]. Thus the vibrational spectroscopic report on excited photodynamics involving ESPT in GFP is very limited [2]. Moreover, it is difficult to find Raman measurements of wtGFP due to the higher degree of complexity involved in its photodynamics than the spectroscopically simpler mutated counterparts. Even though the vibrational Raman markers for the dominant A-(protonated) and B-(deprotonated) forms of the chromophore have been confirmed [15, 19, 20], but any Raman marker associated with the thermodynamically unstable I-form of the chromophore at room temperature has not yet been reported. A probable explanation may involve the extensive use of these isolated analogues of the GFP chromophore, which do not show the similar proton transfer dynamics upon photoexcitation [19]. But it is very important to consider the chromophore embedded inside the protein structure to fully reveal the complex excited state dynamics. Further, a better understanding of the "Förster cycle" (i.e. ESPT) investigated under vibrational spectroscopy will enable the development of a "molecular photoswtich".

The present thesis work reports the first assignment of a unique Raman vibrational marker for the I-state of the GFP chromophore by utilizing single molecule surface-enhanced Raman scattering (SERS). This work successfully exploits the novel "nanometal-on-semiconductor" SERS substrates developed by Kalkan *et al.* [21, 22]. In addition, our experiments show that this I-state is dominantly observable in a cis-configured chromophore implying the fact that the A-form of the GFP population has indeed been excited. This

observation further confirms the modification of the resting times of A and I-states in the "Förster cycle" by utilizing induced SERS conditions.

This work is unique in its sense that no earlier report could be found according to the best of author's knowledge which assigned any vibrational Raman markers for this highly unstable I-state. Previous reports only include picosecond time-resolved infrared absorption [14] and femtosecond stimulated Raman spectroscopic measurements [23] in wt GFP to understand the complex transient skeletal motions involved in the proton transfer and focused on definitively recognizing the proton acceptor. Thus this thesis work not only provides a new Raman marker for the I-state, but also reports such finding at the single molecule level. Habuchi *et al.* and Singhal and Kalkan reported single molecule SERS of EGFP and PYP respectively, but their work studied only the conformational changes of the chromophore states [20, 24]. This is the first reported vibrational spectroscopic document that monitored the ESPT dynamics (i.e. "Förster cycle") of single wtGFP molecules by probing into the native A-state to observe the appearance of a unique Raman peak at a high time resolution of 100 ms.

At this point, it is of particular importance to explain the reasons behind employing SERS instead of normal Raman spectroscopy. At first, SERS inherits the same capability as Raman spectroscopy to elucidate molecular structure with great detail [25]. Raman spectroscopy has been proved to be a great tool for analyzing molecular structures as the spectrum purely consists of molecular vibrational modes. But SERS offers a number of advantages which make it particularly suitable for studying the presented photodynamics of wtGFP. First, GFP is strongly fluorescent even far from the resonance and introduces a strong base line. Thus it is very difficult to clearly resolve Raman peaks. But this fluorescence is efficiently quenched in SERS due to GFP to nanoparticle energy transfer [26-29]. The buried vibrational modes can now be clearly resolved. Second, SERS is used as a probe to facilitate single molecule detection. Single molecule spectroscopy is greatly advantageous over ensemble-averaged spectroscopy (i.e. Raman

spectroscopy) as the statistical averaging gets eliminated [29]. Indeed SERS measurements at high solution concentrations yield a broad and difficult to resolve spectrum due to the overlap of signals from different state populations [30, 31]. But, sharp and clearly resolvable peaks are acquired during SM-SERS measurements. The main advantage of the single molecule spectroscopy lies in the fact that state dynamics of the molecule can be precisely monitored, as a single molecule can only rest at any one of the states at a given time. Thus SM-SERS holds a high potential to probe the excited state dynamics of GFP in great details to reveal underlying transitions involved during ESPT. In particular, SM-SERS is suitable to probe the dynamically fast "Förster cycle" of GFP and observe the highly unstable I-state at room temperature.

Finally, it is necessary to introduce the significance of the present work in relation to the proteins. Proteins are virtually involved in all cell functions. They are the most essential workforces that keep the living cells properly functional. The role of proteins is multifaceted; that involves structural support to bodily movement and defense against germs to sense stimuli, control metabolism and many more. Thus it is very important to fully understand the conformational relations that drive all these protein mediated cell functions. Single molecule studies hold immense potential to greatly aid such understanding.

The present thesis work is organized by the following manner. Chapter II reviews in detail the molecular structure and excited state dynamics of GFP together with the fundamentals of Raman scattering and SERS. Chapter III introduces the detailed experimental protocols that have been followed throughout the current study. The experimental results with their analysis and interpretations are presented and discussed thoroughly in Chapter IV. At the end, important conclusions are established in Chapter V.

CHAPTER II

LITERATURE REVIEW AND BACKGROUND

II.1. Outline

This chapter introduces a comprehensive literature review on Green Fluorescent Protein's molecular structure and photophysics. It also reviews the fundamentals of surface enhanced Raman scattering.

II.2. Molecular structure and photophysics of Green Fluorescent Protein

In 1961 Shimomura *et al.* discovered aequorin and Green Fluorescent Protein (GFP) as a consequence of elucidating the bioluminescence mechanism of the jellyfish *Aequorea victoria*, found in the Northeastern Pacific [32]. This surprise discovery of GFP came while it was isolated as a by-product of aequorin, a luminescent substance, due to its noticeably bright green fluorescence under ultraviolet light [32]. Davenport and Nicol first described the green fluorescence of this jellyfish in 1955 [33], but Shimomura *et al.* [32] found that this green fluorescent substance was a protein. Extraordinarily, this bioluminescent jellyfish glows 'green' *in vivo* due to the presence of the companion protein GFP, whereas pure photoprotein aequorin extracted from the same organism emits 'blue' light upon addition of Ca^{2+} [34]. The emission of 'blue' light from aequorin involves a common enzyme reaction responsible for bioluminescence, termed as luciferin-luciferase reaction, in which luciferin reacts with oxygen to produce light

and the product is catalyzed by the enzyme luciferase. Aequorin (luciferase) has coelenterazine-2-peroxide [35] (luciferin) as the chromophore, shielded centrally by the protein [36]. Two Ca^{2+} ions (co-factor) bind to aequorin and cause conformational changes of the outside protein part, which oxidizes coelenterazine-2-peroxide into coelenteramide and CO_2 with an emission of 'blue' light (470 nm) [34, 35, 37]. Interestingly, GFP absorbs this 'blue' light to produce the characteristic 'green' (509 nm) fluorescence of the jellyfish [1, 34, 35, 37]. Also efficient energy transfer between these proteins does not require any specific manner of binding [34]. Thus to clearly understand if this energy transfer is radiative or radiationless in nature, Morise *et al.* coadsorbed aequorin and GFP on DEAE- cellulose (Diethylaminoethyl cellulose) or DEAE-Sephadex apart from their experiments in solution [34, 38]. It is thus suggested that efficient radiationless energy transfer (Förster type) becomes workable when the distance between these protein molecules become short enough (roughly 30 Å) [34, 38]. After these experiments, involvement of Förster type mechanism is accepted for this protein-protein energy transfer *in vivo* as well as *in vitro* [38]. The discovery of this esoteric protein, GFP, came as a result of an outstandingly basic research of understanding the photophysics of *Aequorea* bioluminescence and did not hold any particular importance at the time of their discovery. But, with the course of time, aequorin became important as a calcium probe and GFP gained wide use as a marker protein [1, 32, 37]

Wild type green fluorescent protein (wtGFP) is a spectroscopically intriguing globular protein having a molecular mass of 27,000 Daltons [39]. Even though many GFP mutants with different spectral properties than wtGFP have been developed, their structural features remain surprisingly similar. GFP was first crystallized in 1974 [38] but the structure was first solved independently in 1996 by Ormö *et al.* [5] and Yang *et al.* [6]. GFP consists of 238 amino acids forming a unique barrel like outside cylinder with an 11-stranded β-sheets, which is run diagonally by a single α-helix (Figure II.1a, b) [1, 5, 6]. This nearly perfect cylinder is about 42 Å

8

in length and 24 Å in diameter [5, 6]. The chromophore, 4-(p-hydroxybenzylidene)imidazolin-5-one [40, 41], is protectively located almost in the center of the cylinder and attached to the α-helix (Figure II.1c) [5, 6].The chromophore plane is poised almost perpendicularly (60°) to the symmetry axis of the surrounding cylindrical motif of amino acid residues [5]. The chromophore is formed from the central helix due to spontaneous cyclization and oxidation of the residues 65-67, which are Ser-Tyr-Gly in the native protein and does not require any external cofactors [1]. The cavity containing the chromophore has a surprising number of adjacent polar groups and structured water molecules [1, 6]. It is accepted that, the robust cylindrical fold of protein is responsible for its stability and bright fluorescence with an exceptionally high quantum yield (ratio of absorbed to emitted photon) of 0.72-0.85 [1, 42]. It is found that fluorescence is completely lost in denatured GFP but can be regained with the refolding of β-sheets into the cylindrical form [43, 44]. This tightly knitted β-sheets with regular pattern of extensive hydrogen bonds act like a highly protective 'jar', which encapsulates the chromophore from the bulk solvent thus avoiding quenching of fluorescence by oxygen and giving it resistance to unfolding by wide range of pH (5-12), heat (i.e. denatures with a loss of 50% of fluorescence at 78℃) and denaturants (i.e. stable even at 8M urea) [1, 6, 39].
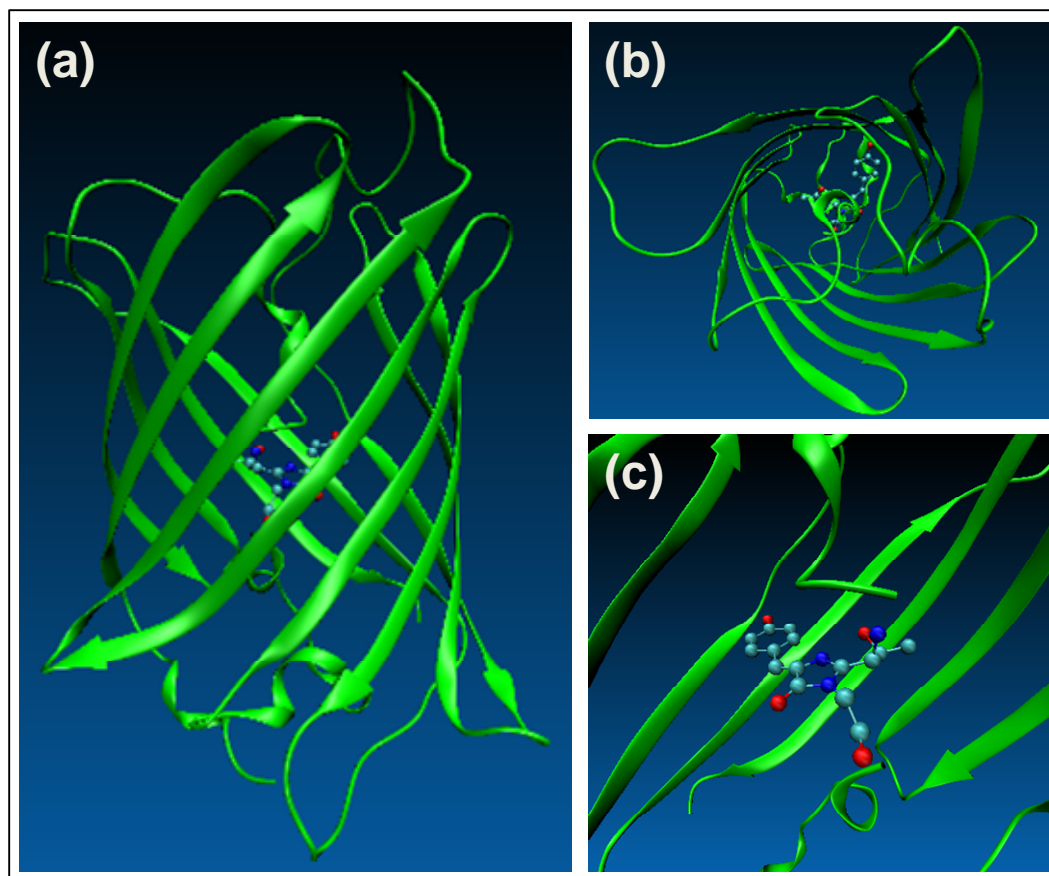
Figure II.1. Three dimensional structure of wtGFP with the chromophore, 4-(p-hydroxybenzylidene)imidazolin-5-one, located centrally inside the folded β-sheets (a) side view, (b) top view, (c) ball stick model of the chromophore (red: O, blue: N, cyan: C), Protein Data Bank accession number 1EMA [1, 5].

Besides encapsulating the chromophore and inhibiting fluorescence quenching by molecular oxygen, the 'jar'-like protein structure also creates barrier to non-radiative conformational relaxation pathways that might otherwise become dominant in the excited state, resulting in a loss of fluorescence [8]. In ground state, GFP chormophore has an extensive π-conjugation due to a relatively planar structure, even though the protein pocket is not complementary with a planar chromophore [8, 45]. This suggests that, the amino acid residues surrounding the chromophore not only exert a steric strain and slightly twist it away from planarity; but also forces the chromophore from rotating freely out of this twisted planarity and

adopt a completely perpendicular conformation in the excited state [8]. When GFP is excited then the extended π-conjugation across the ethylenic bridge between two rings (phenol and imidazolinone) is reduced and the rings can rotate; however this rotation is inhibited by the surrounding protein matrix and thus fluorescence quenching nonadiabatic crossing is prevented [8]. Apart from the planarity, wtGFP chromophore is consistently found to be in a cis configuration, with no substantial evidence of trans-planar configuration in the crystal structure [5, 7]. Even though ground state wtGFP has cis configuration, but photoinduced experiments for HBDI (4-hydroxybenzylidene-1, 2-dimethylimidazoline), a synthetic model of wtGFP chromophore, suggest a volume conserving cis-trans isomerization (Figure II.2) by means of a hula twist type motion leading to a photoinduced trans-planar configuration [8, 46].
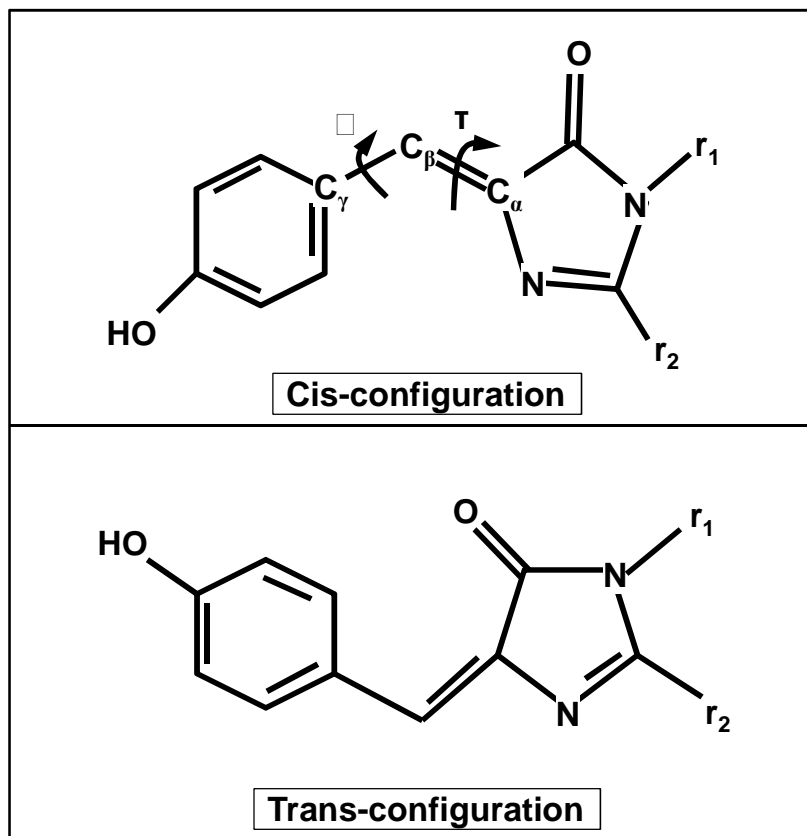
Figure II.2. Schematic of GFP chromophore in the cis and trans-configurations. r_1 and r_2 are the connections with the surrounding protein environment. τ and □ are the two dihedral angles[47].

The photophysics involved in wtGFP is both rich and complex. The absorption spectrum of wtGFP consists of two peaks. A major peak at 395 nm and a minor peak at 475 nm associated with the neutral/protonated and anionic/deprotonated form of the chromophore respectively (Figure II.3) [1, 7, 17, 48]. X-ray crystallographic studies, spectroscopic measurements and studies of pH on model chromophore (HBDI) confirmed the existence of the protonated and deprotonated states [2, 7, 17, 48]. Before illumination with UV light, wtGFP population is present in a 6:1 ratio of protonated to deprotonated forms [1, 10]. Exciting either of the two bands leads to a green emission maximum either at 503 nm (475 nm excitation) or 508 nm (395 nm excitation) (Figure II.3) [1]. Continuous irradiation with UV light decreases the high energy band (395 nm) with a concomitant increase in the lower energy band (475 nm) and this photoconversion is partially reversible, as the initial absorption intensities can significantly be
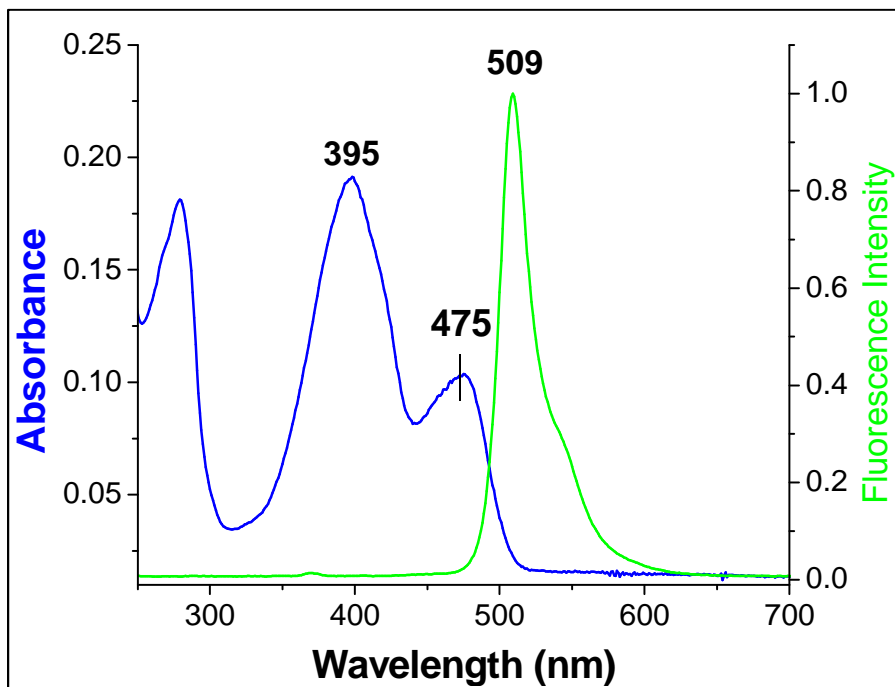
Figure II.3. Absorbance (1 cm optical path) and normalized fluorescence (under 365 nm excitation spectra of 10^{-5} M wtGFP solution.

regained after 24 hours in dark [49, 50]. Interestingly, prolonged excitation at 478 nm also increases the lower energy (475 nm) band with a decrease in the absorbance of high energy band (395 nm) suggesting some overlap of these two bands even at low energy [10].

The most illuminating discoveries regarding the remarkable photochemistry of GFP involves the chromophore acting as a photoacid in its photoexcited state to trigger an ultrafast excited state proton transfer (ESPT), which is responsible for the large Stokes shift in the fluorescence emission [51]. Chattoraj *et al.* reported the excited state dynamics of wtGFP by exciting each of its two strong absorption bands using fluorescence upconversion spectroscopy [10]. Time resolved fluorescence data showed that room temperature excitation of the protonated species (A) at 398 nm creates an excited protonated state (A*) with an emission at 460 nm, which decays with time constants of 3.6 and 12 ps to give corresponding rise of the emission at 508 nm on a similar picosecond timescale [10]. As photoconversion of protonated form (A) into deprotonated form (B) through an excited protonated form (A*) is not an efficient process (large barrier), Boxer and co-workers thus suggested that an intermediate state (I) is present giving rise to an efficient and rapid photoconversion via an excited intermediate anion (I*) involving ESPT [9-11]. This kind of excited state protolytic reaction, where an excited protonated species (RH*) form an excited anion (R⁻*) is very common in solution photochemistry since its discovery by Theodor Förster in 1949 [9]. Thus, upon photoexcitation the protonated form of the chromophore (A) forms an excited protonated state (A*), which quickly losses the proton to form phenolate (anionic) chromophore from the phenolic (protonated) chromophore via the extensive hydrogen bonding network including water molecules, residues Ser205 and Glu222 (internal 'proton pathway') (Figure II.4) [7, 50, 52, 53].
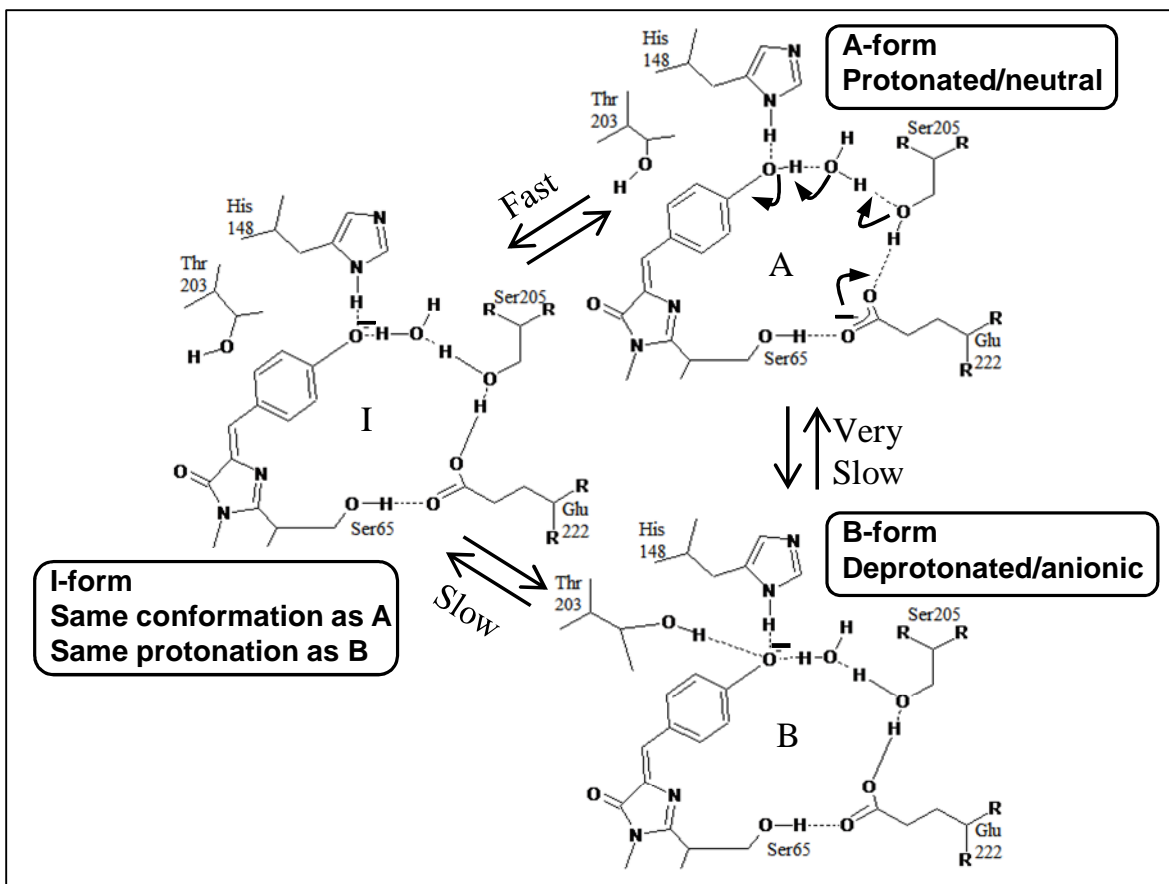
Figure II.4. Suggested photoconversion mechanism of the A and B forms of the GFP chromophore through I state. The conversion from protonated (A) form to the anionic (B) species involves phenolic proton movement of Tyr66 via an extended hydrogen bonding to the carboxylate oxygen of Glu222. Arrows indicate the internal 'proton pathway' in opposite direction [50, 53].

The excited state, A*, converts to an excited intermediate anion (I*) and relaxes back to the intermediate ground state (I) with a relaxation time of 3 ns by giving green emission at 508 nm [10, 11, 53]. After relaxation to I, subsequent re-protonation of the chromophore reforms the photoconverted protonated ground state (A) on a time scale of 400 ps and completes the relaxation cycle (A→A*→I*→I→A) by involving an internal proton movement (i.e. Förster cycle) through potential proton acceptors around Tyr66 of the chromophore [9, 10, 52, 53]. A schematic of this excited state dynamics of wtGFP involving the "Förster cycle" is illustrated in Figure II.5 a, b respectively. Although wtGFP has a unique structure shielding the chromophore

from the bulk pH of the solution, an exceptional 'proton pathway' of water molecules and internal residues run from Glu222 (proton acceptor) to Glu5 at the bottom of β-structure facilitating external proton translocation out into the bulk solvent [7, 14, 18, 54]. Alternatively, rotation of Thr203 could also promote external proton translocation onto the backbone carbonyl (C=O) of His148 and from there, out into the bulk solvent [52, 55]. Even though photoconversion of A*→I* is facile, the non-radiative conversion from I*→B* is slow and happens infrequently via a rotation of Thr203 [50, 56]. Irradiation of the deprotonated state (B) of the chromophore at 475 nm directly creates an excited anion (B*), which emits at 503 nm and does not involve ESPT [10]. Similarly, reported emission maxima of I→I* (508 nm) and B→B* (503 nm) indicates two deprotonated and structurally similar excited states with ground state of I being considered as an unrelaxed form of B having a lower degree of H-bond stabilization at phenolic oxygen [7, 10, 56, 57]. Creemers *et al.* confirmed that I-form of the chromophore is indeed populated at room temperature using spectral hole-burning spectroscopy and found the absorption maxima for this intermediate ground state at 495 nm [12].
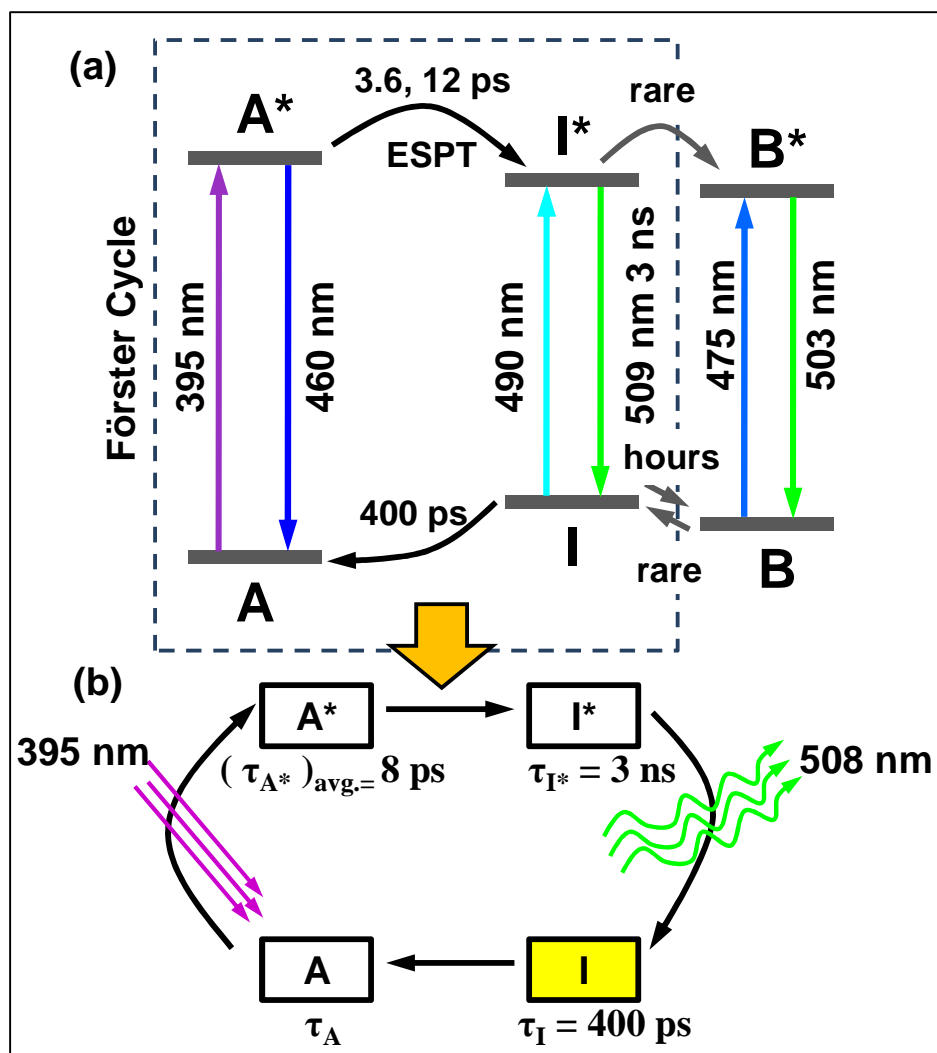
Figure II.5. Schematic of (a) summarized photodynamics of wtGFP showing (b) the "Förster cycle" with associated inhabiting time of each state [7, 11, 53].

II.3. Fundamentals of Surface Enhanced Raman Scattering (SERS)

In 1928, the Indian physicist C. V. Raman discovered the effect named after him [58, 59]. The theory behind this inelastic scattering of photons was first predicted by Adolf Smekal in 1923 [60]. In Raman effect exchange of energy occurs between the molecules and the incident photons; and this difference in energy corresponds to the energy of the vibrational and rotational modes of the molecule [58-61]. Stokes lines are generated if the molecule absorbs energy, resulting in a

photon of lower energy and Anti-Stokes lines are generated while the molecule loses energy

resulting in photon of higher energy (Figure II.6) [58, 59, 61, 62].
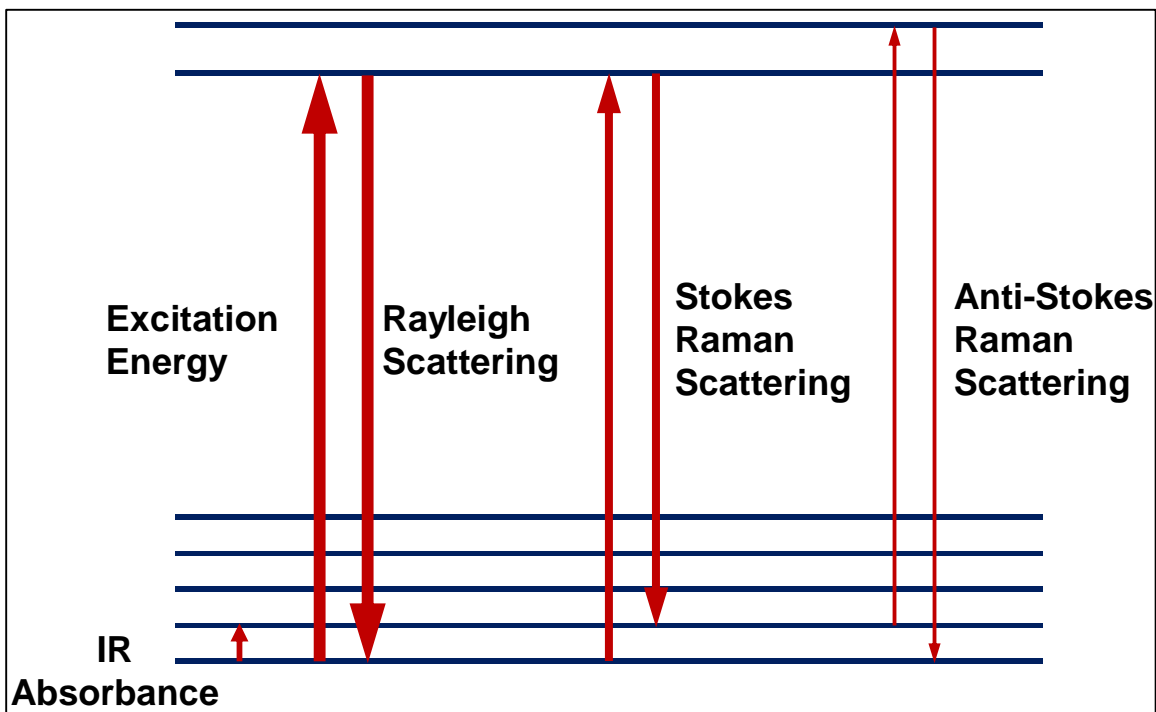
Figure II.6. Energy diagram indicating different process of light scattering. Thickness of the lines indicates the strength of scattering signal associated with different mechanisms.

In recent years Raman spectroscopy is revived as a substantial tool for studying the bio-molecules due to its inherent ability to provide exceptionally detailed information about molecular structure. However, use of Raman spectroscopy is limited as high concentrations of analyte act as an essential pre-requisite due to the small Raman cross sections of the molecules (on the order of 10^{-34} cm^2/molecule) [25, 28, 35, 63, 64]. Despite having very important advantages, Raman spectroscopy lost significant interest to fluorescence spectroscopy, that exploits fluorescence cross sections on the order of 10^{-17} cm^2/molecule [25, 28]. But fortunately enough in 1974 Fleischmann *et al.* [65] first observed dramatically increased Raman scattering from pyridine adsorbed onto electrochemically roughened Ag electrode surfaces, which was later

pointed out by [66] and Albrecht and Creighton [67] as surface-enhanced Raman scattering

(SERS) in 1977 and this exceptional discovery re-established Raman spectroscopy as an

invaluable tool for collecting detailed molecular information compared to fluorescence

spectroscopy [25]. SERS can reportedly achieve a remarkably high enhancement factor in the

order of 10^{14}, which enables detection of single molecules adsorbed on metallic surfaces; but

some revised experiments indicate a more reasonable case of 10^8-10^{11} SERS enhancement factor

[26, 63, 68-70]. Starting from 1980, SERS received dramatic attention in various fields including

electrochemistry, analytical chemistry, chemical physics, solid state physics, biophysics and even

medicine [25, 71, 72]. Ag and Au are commonly used to make SERS substrates [25].

Mainly two mechanisms are associated with SERS effect; a) electromagnetic and b)

chemical, where electromagnetic enhancement (EM) mechanism is regarded as the chief

contributor of SERS [25, 66, 67]. Electromagnetic enhancement involves the enhanced

electromagnetic fields supported on metal nanostructures and a simple understanding of this

mechanism is estimated by examining the electrostatics of a polarizable metal nanosphere present

in a uniform external electric field [25, 66, 67]. This electrostatic approximation for explaining

EM enhancement holds well when the radius of a spherical metal particle is much smaller than

the wavelength of incident light ($r \ll \lambda$) [25]. According to the stated condition, incident plane

wave of light can be considered as a localized dipole field in the center of the spherical metal

particle and this particle with localized light (dipole field) enhances both the incident laser field

and the Raman scattered field with an overall enhancement that roughly scales to E^4 [25]. Thus

incident light excites oscillating dipole fields that are localized and supported on the surfaces of

the metal nanostructures. These collective oscillations of electron gas cloud (dipole fields) are

called "plasmon resonances" and if these oscillations are confined near the surfaces of the

metallic nanostructures then they are described as "surface plasmon (SP) resonances" [25, 72,

73]. Strong EM field created by these SPs couples with the adsorbed molecule and facilitates

Raman scattering. The adsorbed molecules scatter the EM field and produce a new field with a shifted frequency due to Raman process, that may be further enhanced by the interaction of metal with the molecules [25, 73]. This enhancement becomes particularly strong in between the nano-gaps of the metallic nanoparticles (NP) with an optimum distance of 1 nm [74].

Metal-molecule "charge transfer" (CT) responsible for an additional enhancement typically by factors of 100 to 10000 is an independently operating "chemical enhancement" mechanism secondary to the EM enhancement [25, 75]. Although EM enhancement serves as a nonselective enhancer for Raman scattering by all molecules adsorbed on a particular surface, yet smaller but significant enhancement is observed as a result of charge transfer from the molecule to the metal surface or vice versa [25, 75, 76]. The CT enhancement mechanism is restricted to the fact that the molecules have to be adsorbed directly on the metal and this condition is not required by the EM effect which can extend to a certain distance beyond the surface [73, 76]. Lombardi and Brike developed a theoretical framework for analyzing CT effects and obtained expressions for Raman polarizibility taking into account the possible electronic transitions involving CT between the molecule and metal [75]. In this theoretical framework resonance Raman process is considered to be the main contributor of CT transitions leading to the enhancement of Raman spectra, which is later experimentally demonstrated by Haran [73, 76]. Coinage (Ag, Au, Cu) and alkali (Li, Na, K) metals NPs are primarily used as SERS substrates due to their exhibition of localized SP resonances/excitations in the visible range which is particularly important for probing dyes and bio-molecules with Raman spectroscopy [25, 63].

In 1997, Kneipp *et al.* first reported the observance of highly enhanced Raman scattering with exceptionally large Raman cross sections ($10^{-17} – 10^{-16}$ cm^2/molecule) from SERS while measuring Raman spectra of single crystal violet molecule in aqueous solution of colloidal silver [63]. In the same year, Nie and Emory in their breakthrough paper, demonstrated single molecule (SM) SERS from rhodamine 6G (R6G) molecules adsorbed on Ag nanoparticles exhibiting an

unusual Raman enhancement factor on the order of 10^{14} to 10^{15} [28]. Nie and Emory [28] followed an extensively time consuming procedure as described by Lee and Meisel [77] to prepare Ag colloid solution and successively incubated an aliquot of R6G molecules for ~3hours at room temperature to facilitate analyte adsorption [28]. After that, these analyte adsorbed Ag particles (heterogeneous particles with an average size of about 35 nm) were immobilized on polylysine coated glass surfaces prior to SERS [28]. Majority of these immobilized Ag nanoparticles are found to be well separated single particles, but a minor fraction was found to consist of aggregates and this phenomenal discovery by Nie and Emory opened the possibility of SM detection [28].

SM-SERS is exciting as a tool to gain detailed information about molecular dynamics in heterogeneous media, from living cells to chemical catalysts [25, 28]. SERS sample preparation in this method involves extended procedures to ensure that very few molecules preferably one molecule get adsorbed per particle on an average and thus this technique found limited use [28].

The present thesis work adopts and follows a unique approach developed by Kalkan *et al.* [21, 22, 24] for SM SERS measurements including preferentially added modifications. This specific approach is found to be a more efficient alternative than that followed by Nie and Emory [28]. Preparation of SERS substrates require less time and the experimental procedure is simple and straightforward. Chapter III provides detailed information about the experimental protocols followed in this thesis.

CHAPTER III

EXPERIMENTAL DETAILS

III.1. Outline

This chapter presents the details of experimental measurement conditions and protocols that are employed in the detection of single GFP molecules. It also provides detail methodology for fabricating the "nanometal-on-semiconductor" SERS substrates that exhibit a reproducible high SERS enhancement for single molecule detection.

III.2. Semiconductor thin film deposition

Monolayer of silver (Ag) nanoparticles were chemically reduced on thin germanium (Ge) films to fabricate the "nanometal (Ag)-on-semiconductor (Ge)" SERS substrates [21, 22]. Ge thin film immobilizes the Ag nanoparticles in addition to serving as the reducing agent for nanoparticle synthesis. The Ge reducer thin films were deposited on 2" × 1" Corning 1737 code glass slides. A set of extensive cleaning protocols were developed and strictly followed for the glass slides before depositing Ge thin films. This strictly maintained set of cleaning procedures was necessary to get rid of all foreign particles as well as organic residues from the glass surface. Glass slides were immersed in a 300 ml solution of 50% IPA (isopropyl alcohol), containing 125 ml DI (deionized) water and 125 ml of 99% pure IPA solution. After the immersion, a soft

brush was used to scrub off any organic residues and particles. The immersed glass slides in 50% IPA solution were then ultrasonicated for 15 min. at a temperature of 70°C to remove adsorbed impurities. After the ultrasonication, glass slides were taken out of the 50% IPA solution and rinsed thoroughly with DI water. An additional 5 min. of ultrasonation was employed by immersing the cleaned glass slides in DI water to remove all IPA residues. Subsequently, the glass slides were blow dried with nitrogen/argon before putting them on a hot plate at a temperature of 150°C for 15 minutes to desorb the moisture from the glass surface.
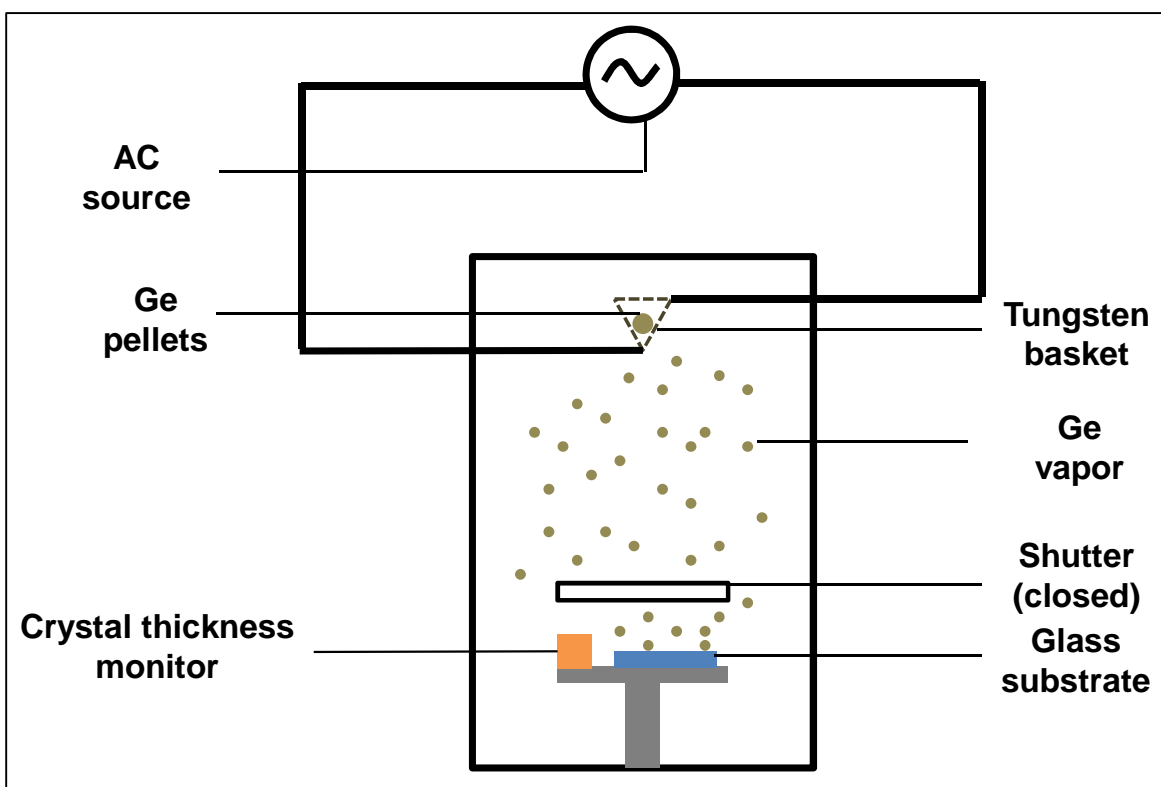
Figure III.1. Schematic of PVD system employed to deposit thin Ge films on glass substrates.

A Cressington 208 Carbon High Vacuum Turbo Carbon Coater was utilized as the Physical Vapor Deposition (PVD) system to deposit the thin Ge films on the glass slides and the schematic of the PVD process is depicted in Figure III.1. As depicted in the figure, cleaned glass slides were placed on the deposition platform under the shutter, and Ge pellets were loaded in the

small tungsten-wire basket. To achieve a base vacuum pressure of 4×10^{-5} mBar inside the deposition chamber, a turbo pump backed up by a mechanical pump was employed. Ge pellets were melted by the resistance heating inside the small tungsten-wire basket as electric current is adjustably increased through it. Density was set to 5.32 g/cm^3 for Ge in the crystal thickness monitor before achieving a pre-decided deposition rate of 2.5 Å/s by gradually adjusting the current through the basket. Then the crystal thickness monitor was set to zero before opening the shutter to let the deposition of Ge on the glass slide start. The shutter was kept open to coat a film of 4.5 nm thickness in approximately 18 s. Subsequently, shutter was closed and gradually current was decreased to zero. The deposition chamber was allowed to cool down under the base vacuum pressure for an added 15 minutes before it was vented and deposited Ge substrate was removed.

III.3. SERS substrate fabrication by nanoparticle reduction

After depositing 4.5 nm thick Ge film on glass slide, it was immersed in 0.002 M AgNO$_3$ solution for 22 to 25 s to reduce Ag nanoparticles on the surface, thus producing SERS active substrate. A schematic of the reduction process employed to prepare these SERS substrates is depicted in Figure III.2.
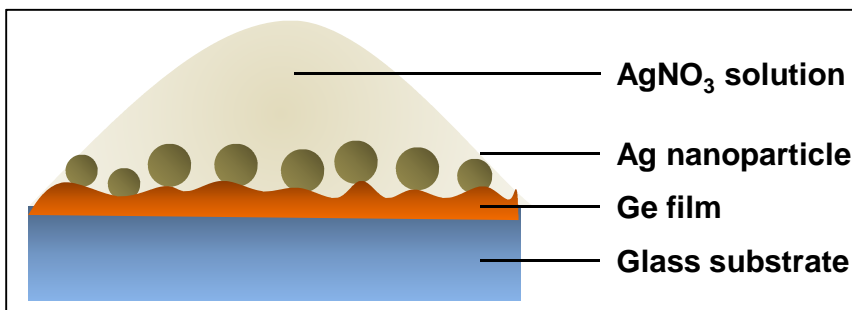
Figure III.2. Illustration of the Ag nanoparticle reduction process on Ge thin film to fabricate SERS active substrates.

Absorption of the SERS substrates was measured using Cary 300 UV-Visible spectrometer after reducing Ag nanoparticles. Absorption measurement was employed as a diagnostic tool for checking the reproducibility of the SERS substrates before starting the SM-SERS acquisitions.

III.4. Acquisition of SM-SERS spectra

A WITec alpha300R system equipped with a confocal microscope was used to perform SM-SERS measurements. A 532 nm Nd:YAG (neodymium-doped yttrium aluminium garnet; Nd:$Y_3Al_5O_{12}$) laser was employed as the Raman excitation probe. A grating of 600 g/mm was used as the default grating. Typically, a 1μL aliquot of 1 x 10^{-9} M solution of wtGFP was spotted on the SERS substrate prior to the SM SERS acquisition. Subsequently, the substrate was sealed inside a spectrometer cell (Starna cell, 12.5 x 3.5 x 45 mm^3) with a small piece of wet wipe. Wet wipe prevented quick drying of the aqueous aliquot after reaching thermodynamic equilibrium and facilitated SM SERS acquisition from the same spotted aqueous aliquot for a relatively long period of time without repeated necessity of spotting the aliquot. Figure III.3 graphically demonstrates the setup for the acquisition of the SM SERS spectra.
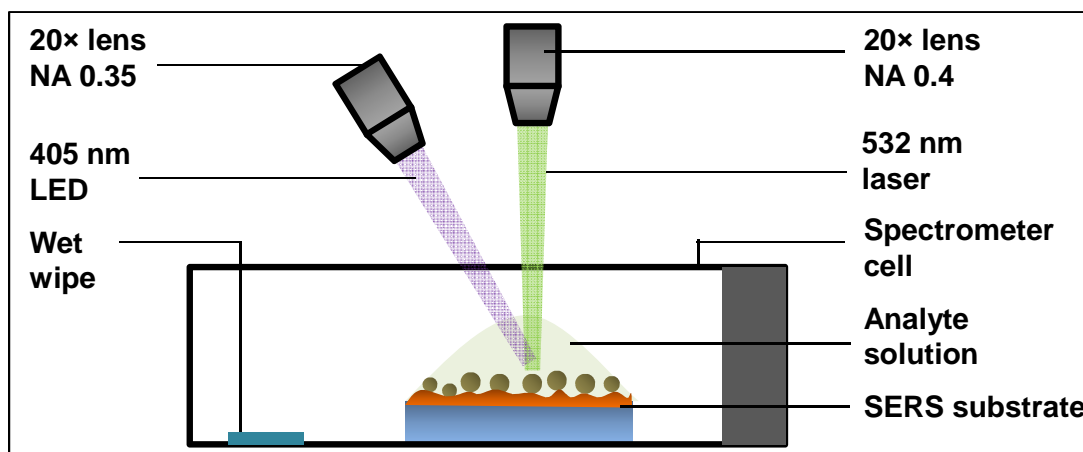
Figure III.3. Illustration of SM-SERS acquisition using 532 nm as the Raman probe laser and 405 nm LED excitation as the pump.

An objective lens of 20× (NA 0.4) was utilized for focusing the 532 nm Raman excitation probe at the aliquot-substrate interface and as well as for collecting Raman signal. Laser spot size was fixed at 2 μm and the incident power was set to ≅100 μW. To excite the native protonated population of wtGFP, A-state, we employed an external LED source (405 nm, fixed at constant output power of ≅ 30 mW). The LED radiation was focused at the Raman probe spot for pumping using another 20× objective lens (NA 0.35) and no signal was collected using this objective lens. The external LED source utilized for pumping purpose is a Prizmatix fiber coupled triple wavelength LED source. A custom designed positioner was fabricated to hold and effectively position the other 20× objective lens, which had a built-in collimator with SMA fiber optic connection output to securely couple the 405 nm LED source. Once the excitation was turned on, SM-SERS acquisition was started at an integration time of 100 ms.

CHAPTER IV

RESULTS AND DISCUSSIONS

IV.1. Outline

This chapter focuses on presenting and analyzing the time series SERS spectra of single GFP molecules. A new Raman peak, suggested as the marker for I-state, is dominantly observed to appear as a result of nanoparticle-enhanced optical pumping by 405 nm external LED source under the 532 nm Raman excitation. This never before reported Raman marker is found to be prominently present together with the protonated Raman marker of GFP. Interestingly, in absence of 405 nm LED excitation, this new peak is not observed (spectra not included). Previous work in the group with wtGFP employing only 532 nm Raman probe laser never observed the appearance of this particular new peak [78]. Probability of finding the protonated marker given the presence of this new Raman peak is investigated extensively. In addition, the correlation with this new marker and the 4 conformational states of GFP is also analyzed. Cis-protonated (A-form) state is observed to appear with this new marker more profoundly than other states. All the conditional probability results are presented in the form of 3D histograms at the end of this chapter.

IV.2. Collection of SERS spectra from single GFP molecules

1 µL solution of 1×10^{-9} M GFP was spotted on the SERS substrate before starting the acquisition of SERS spectra. The Raman excitation probe (532 nm laser) was focused through a 20× lens at a spot size of 2 µm at the aliquot-substrate interface. Concurrently, the external LED source (i.e. pump, 405 nm) was also focused using another 20× lens on the same spot. After that, time series SERS spectra were collected by simultaneously starting both the Raman excitation probe and the pump by setting an integration time of 100 ms. Noticeably strong and clearly resolvable Raman peaks started to appear on the weak background once every 30-35 seconds, on average. These evidently strong and clearly resolvable spectra are temporal in nature and appearance of one such series of spectrum is collectively referred as 'spectral jump'. One 'spectral jump' is sustained for about a second on the average. These spectral jumps are associated with a single GFP molecule diffusing in and out of a high SERS enhancement site supported on the "nanometal-on-semiconductor" substrates. These sites with highly enhanced electromagnetic fields, sustained on the metal nanostructures, are commonly known as "hotspots" and facilitate single molecule detection [25, 28, 63, 79].

There are several key evidences, as mentioned and accepted in the literature, required to be analyzed to confirm that the aforementioned spectral jumps indeed arise from single GFP molecules adsorbed on these "hotspots" and such evidences are presented and discussed in the following section. Figure IV.1 illustrates a representative time series SERS spectral jump associated with a single GFP molecule being adsorbed at a "hotspot".
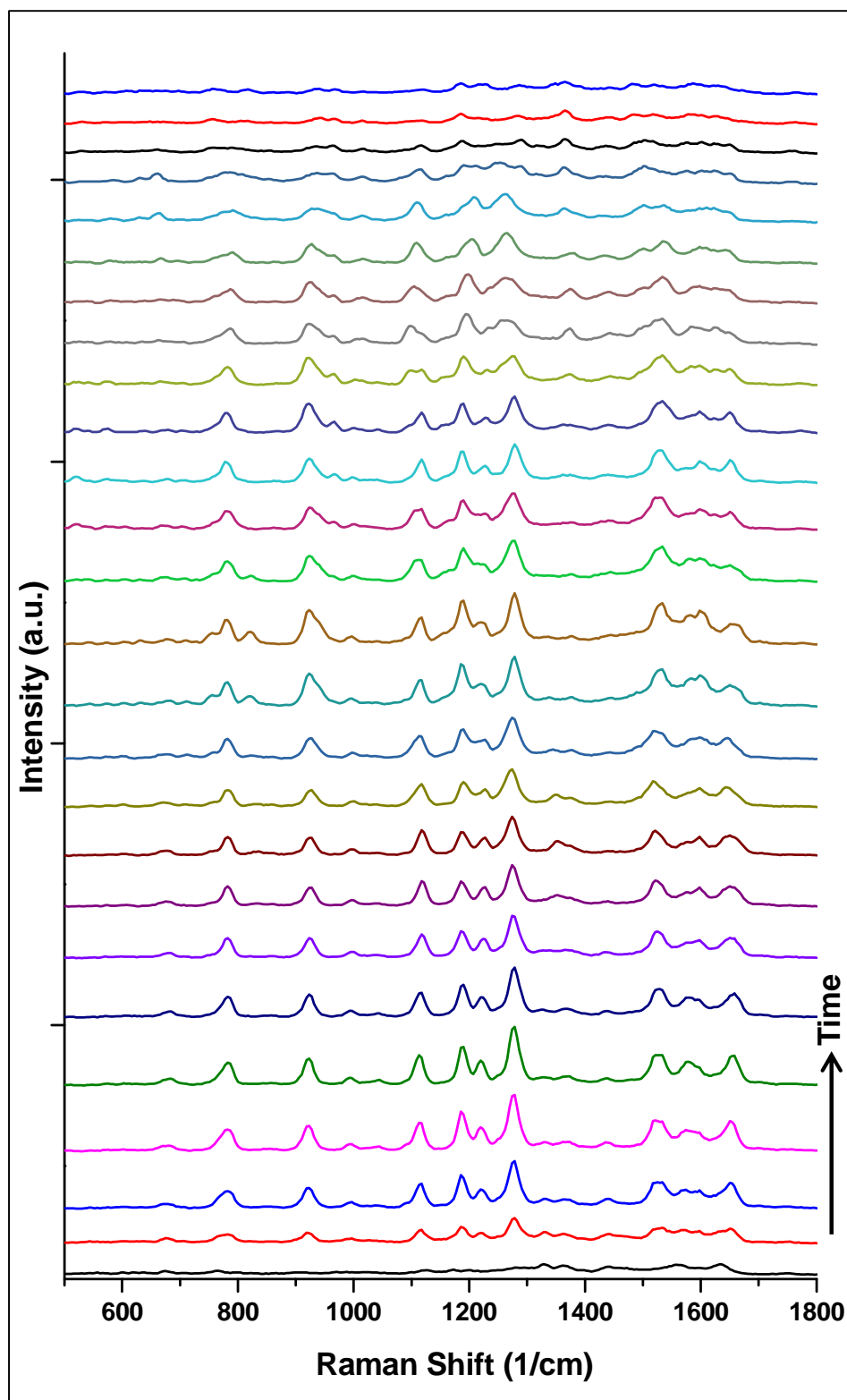
Figure IV.1. Time series SERS spectra of a single GFP molecule demonstrating a "spectral jump" at time intervals of 100 ms and 100 μW laser power.

IV.2.1. Minor temporal fluctuations in spectral wavenumbers

Minute analysis of the spectral jump provided in Figure IV.1 reveals minor fluctuations in the spectral wavenumbers with time. Raman peaks undergo random and temporal shifts, within a range of ± 5 cm^{-1}, in consecutive spectra. This evidence is exhibited clearly in Figure IV.2 (a) These minor temporal spectral fluctuations associated with the consecutive spectra in one 'spectral jump' is considered as an evidence of capturing single GFP molecules.

Charge transfer between the GFP chromophore and the nanoparticle does not occur due to the presence of the protective outer β-fold of the GFP. GFP molecules undergo only a weak adsorption on the surfaces of Ag nanoparticles. Due to this weaker adsorption, GFP can have a certain degree of translational and rotational freedom. Thus the motion of GFP molecules are slowed down, but not totally restricted. This partially inhibited motion of GFP induces stress on the cylindrical structure of β-sheets and slightly alters the bond length and angle of the chromophore located centrally inside the cylindrical motif. As a consequence of this, minor fluctuations in the wavenumber occur with time. These kind of temporal spectral fluctuations were reported earlier as a typical characteristic of single molecule SERS activity [20, 28, 79].
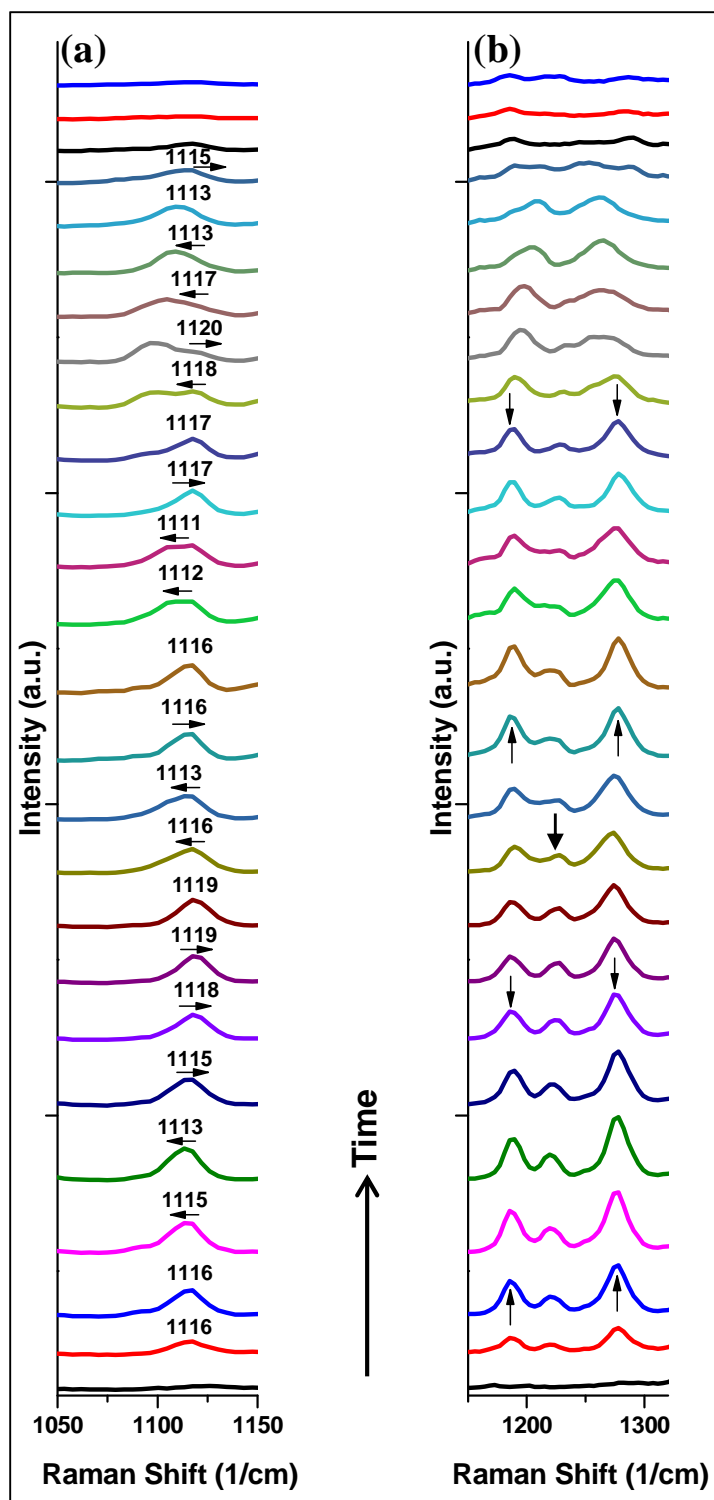
Figure IV.2. Time series SERS spectra of a single GFP molecule showing: (a) randomly occurring temporal fluctuations of a Raman peak (1050-1150 cm^{-1} range of Figure IV.1) and (b) relative intensity fluctuations of the peaks (1150-1350 cm^{-1} range of Figure IV.1). Arrows indicate (a) relative spectral shifts and (b) relative intensity fluctuations in comparison to the previous scans.

IV.2.2. Relative intensity fluctuations of the peaks

Another reported evidence of the single molecule SERS spectra is the presence of relative intensity fluctuations in the Raman peaks [20, 79]. Indeed, such fluctuations in intensity can be observed in the Figure IV.2 (b) A highly enhanced Raman scattered signal becomes detectable when a molecule is adsorbed at a 'hotspot'; but this adsorbed molecule can attain different orientations on Ag surface in time. Such situation can occur with weakly adsorbed GFP molecules. Namely, the GFP molecule rotates or "rolls" on the Ag surface. The surface enhanced field is normal to the Ag surface and surface selection rule essentially implies that only vibrational modes with polarizibility components normal to the surface are enhanced [28, 79].Thus the detected intensity of SERS spectra depends on the alignment of the Raman transition moment of that particular vibrational mode with the surface enhanced field. It means intensity of a particular Raman peak is maximized when that transition moment becomes normal to the surface. The direction of Raman transition moment is also dependent on the molecular orientation as a whole. In addition, different molecular vibrational modes also have different Raman transition moments associated with them. Thus, at some particular orientation on the Ag surface some Raman peaks of GFP can be pronounced with the ceasing of some other peaks. Slightly inhibited rotational motion of the adsorbed GFP molecules can induce such temporal fluctuations in the peak intensities. These relative intensity fluctuations are absent in an ensemble averaged Rama spectrum, suggesting such fluctuations as an evidence of single molecule detection.
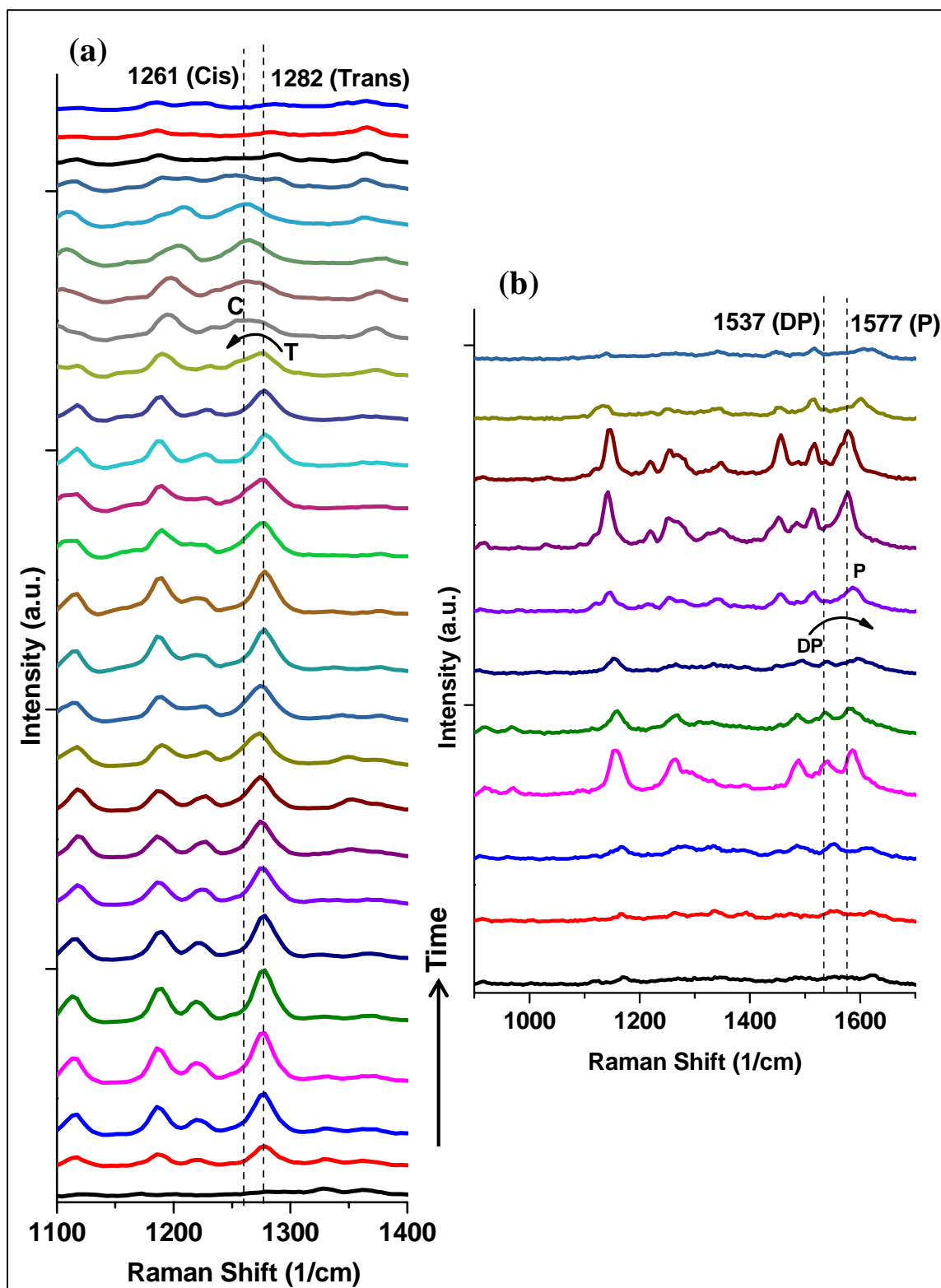
Figure IV.3. Time series SERS spectra of single GFP molecule indicating structural transitions: (a) change in conformational state from trans→cis (1100 -1400 cm^{-1} range of Figure IV.1) and (b) change in protonation state from DP→P.

IV.2.3. Structural transitions

Sudden appearance of one Raman peak with concomitant ceasing of another Raman peak is common to SERS spectra detected from single molecules [20]. Such occurrence is observed in Figure IV.3 (a), where a peak at 1282 cm^{-1}(Raman marker for trans-configured chromophore [80]) gradually ceases to give rise to another peak at 1261 cm^{-1} (Raman marker for cis-configured chromophore [80]) in the next spectra. This phenomenon is attributed to a structural transition in the captured single GFP molecule. Any single molecule can stay only in one single conformational state at a given time. Thus any change in the spectral wavenumber on the order of ± 15 cm^{-1}, unlike minor fluctuations of ± 5cm^{-1}, indicates a change in the conformational state of that molecule. Further, this frequency change is present for a longer time scale, as observed in Figure IV.3 (a), (b). Thus, major frequency change in the consecutive SERS spectra indicates individual molecular activity and provides another strong evidence of capturing single GFP molecules. In case of ensemble averaged Raman spectra, such mutually exclusive peaks cannot be definitively resolved and appearance of such peaks in the same spectra is also observed as a consequence of the existence of populations of different forms. Sometimes, occurrence of two or more structural transitions in a single spectral jump is also possible though not observed significantly under current experimental conditions.

IV.3. Capturing and identifying a new Raman peak in the SM-SERS spectra

A new Raman peak can be consistently observed in the SM-SERS spectra of single GFP molecules under the employed experimental conditions. This new peak is dominantly present with the protonated Raman marker. But found to be absent when single GFP molecules are captured in the deprotonated state. Further evidences will be presented in the later sections regarding this unique peak together with analysis and plausible explanations. The following section summarizes the identifiable Raman markers associated with the different states of GFP to

clearly distinguish between the observed states. This is necessary to initiate a logical understanding of the Raman markers that will be extensively referred in the subsequent sections.

IV.3.1. Identifying Raman markers for 4-different states of GFP

As mentioned earlier, most of the available reports provide ensemble averaged Raman spectra to assign vibrational modes of isolated model chormophore. Based on these reports, 4 Raman peaks can be identified as the markers for 4 different states associated in GFP. At first, it is necessary to introduce these 4-Raman vibrational markers to clearly distinguish between the observed states in the SM-SERS spectra.

GFP is present in two forms of the chromophore: protonated and deprotonated; and conversion between these forms are common [20]. Apart from changes in the protonation states of the chromophore, another possibility involves a non-radiative relaxation process by which the chromophore can undergo a volume conserving cis-trans isomerization inside the protein structure [8]. In the native protein fold, GFP chromophore adopts a cis-configuration as determined by X-ray crystallographic studies [5-7].According to Weber *et al.* [81] trans-isomer is plausible and can stay in the same protein environment as the cis-isomer [81]. But experimentally determined structures show only the cis-configuration of the chromophore and this suggests that trans-configured chromophore is not well supported by the surrounding protein environment, but does not exclude the possibility of cis↔trans transition of the chromophore in the excited state [81]. Thus it is expected that GFP chromophore can reside in these following 4-states: cis-protonated, cis-deprotonated, trans-protonated and trans-deprotonated, though possibility of cis→trans or/and trans→cis transitions is expected to be less compared to the transitions involving protonation.

Habuchi *et al.* reported the ensemble-averaged Raman spectrum of EGFP at neutral (pH =7.4) and acidic (pH=5.0) solutions; and observed two important peaks located at 1536 cm^{-1} and

1556 cm^{-1} [20]. These peaks are attributed to the delocalized imidazolinone/exocyclic C=C mode

of the chromophore as reported by He *et al.* based on isotope labeling and normal mode analysis

of HBDI [16]. This particular mode is dominantly associated with the stretching of C=N bond of

the imidazolinone ring and the C=C double bond linking the two rings and has been referred as

C=N stretch by Esposito *et al.* [19]. Therefore, the peak at 1556 cm^{-1} is associated with the

protonated form of the chromophore, while 1536 cm^{-1} corresponds to the deprotonated form [19].

Later, in 2003, Habuchi *et al.* first reported surfaced-enhanced resonance Raman spectra

(SERRS) of single EGFP molecules adsorbed on Ag particles [20]. Most of the peaks observed in

their SM-SERRS spectra agreed well with an error of ± 10 cm^{-1} [20]. In these SM-SERRS spectra,

Habuchi *et al.* reported 1524 cm^{-1} as the deprotonated form of the chromophore and 1562 cm^{-1} as

the protonated form [20].Based on these reported results of SM-SERRS spectra 1530 cm^{-1} and

1560 cm^{-1} (within a range of ± 10 cm^{-1}) are considered as the deprotonated and protonated Raman

marker peaks, respectively.

In 2006, Loos *et al.* first reported cis- and trans- Raman markers by comparing Raman

spectra of eqFP611 and DsRed [80]. Both of these observed red fluorescent proteins have similar

chromophores like GFP; but the π-conjugation is further extended to modify the emission color to

red [80]. The chromophore of eqFP611 has a coplanar trans-configuration, while the

chromophore of DsRed is present in a coplanar cis-configuration [80]. Preresonance Raman

spectra (752 nm laser excitation) of eqFP611 and DsRed revealed a distinguishable difference in

the range of 1260 -1285 cm^{-1} [80]. A doublet of bands was clearly observable at 1270 cm^{-1} for

eqFP611; and suggested the presence of two different species(cis and trans) in the sample which

is observed to be same as HeRed, another fluorescent protein, that can also be present in either of

the two configurations like eqFP611[80]. Whereas, DsRed preresonance Raman spectrum

indicated only a single band at 1260 cm^{-1} which confirmed the presence of the cis-configuration

in its native state [80]. Irradiation of eqFP611 with a 532 nm pulsed laser essentially

photoconverted all the species to a single form of the chromophore and revealed a single Raman band at around 1260 cm^{-1} [80]. This was an indication that indeed a trans→cis photoconversion had been driven; and Loos *et al.* reported 1260 and 1280 cm^{-1} as the Raman markers of cis and tran-configured chromophore, respectively as a rational outcome [80]. This particular report is valuable in assigning the similar Raman markers for GFP chromophore, as both of these observed red fluorescent proteins have similar chromophores like GFP with only a difference in the π-conjugation [80]. Thus based on this report 1260 and 1280 cm^{-1} have been considered as the Raman markers for cis-and trans-configured chromophore, respectively.

Also this consideration is validated by carefully observing the Raman spectra provided by Bell *et al.* and He *et al.* [16, 17]. Table IV.1 provides all the aforementioned Raman markers as a combination of protonation/deprotonation and cis/trans to introduce the considered Raman markers for the 4 different states of GFP.

	Protonated 1560 cm^{-1}	Deprotonated 1530 cm^{-1}
Cis 1260 cm^{-1}	A	B
Trans 1280 cm^{-1}	C	D

Table IV.1. Raman markers adopted from the literature to identify 4-different states of GFP chromophore.

All of these Raman markers are observed in the SM-SERS spectra of the present thesis work. Figure IV.4 represents 4 separate SM-SERS spectra, where single GFP molecules are captured in these 4 different states. According to the Table IV.1; Figure IV.4 (a),(b),(c) and (d) captured single GFP molecules in A,B,C and D-states, respectively. Interestingly, a new Raman

peak is observed to accompany state A and C at around 1510 cm^{-1}. Further, this particular peak is absent while the GFP chromophore is captured in state B and D.
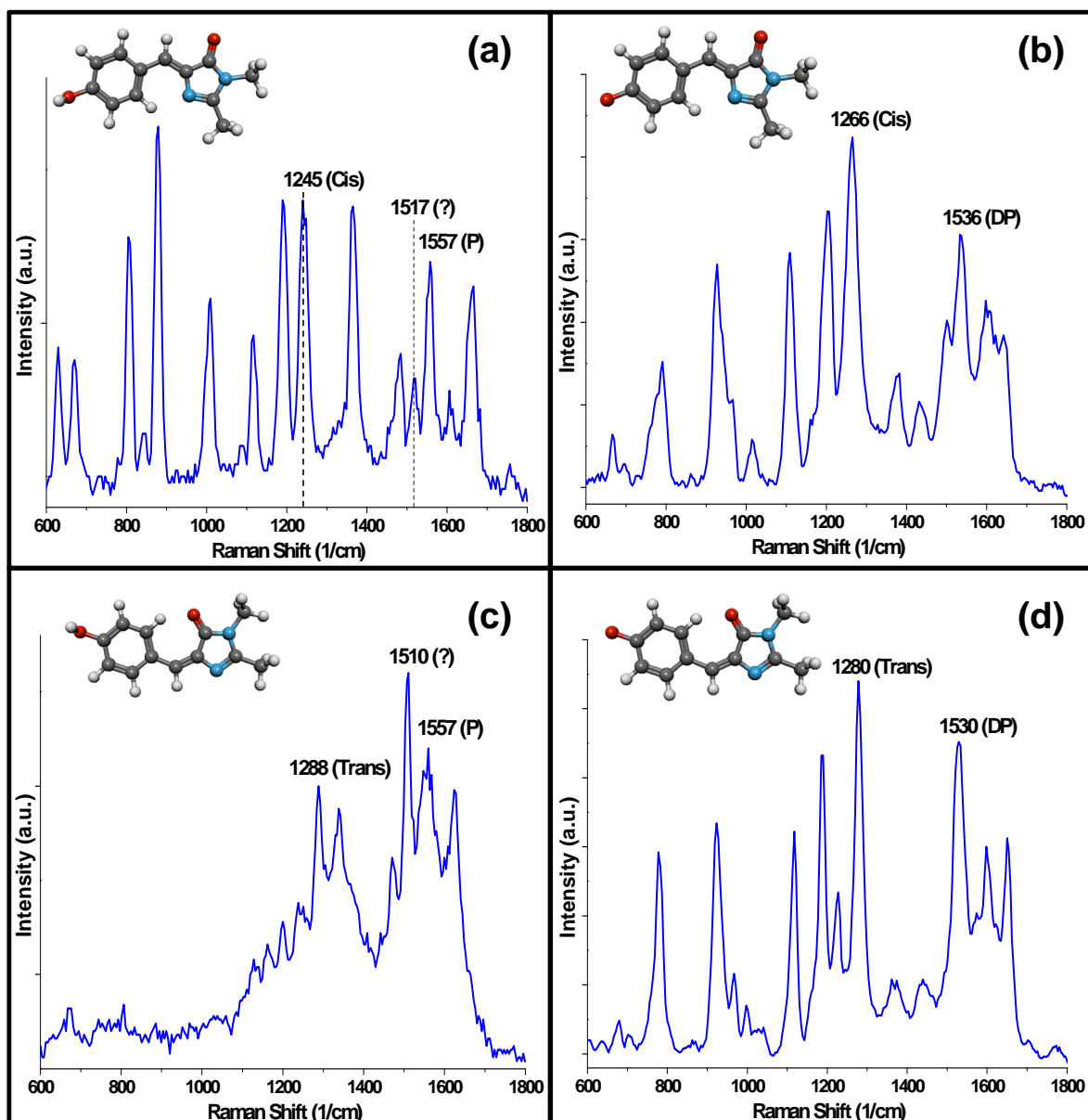
Figure IV.4. SM-SERS spectra captured from individual GFP molecules indicating (a) A state, (b) B state, (c) C state and (d) D state as stated in Table IV.1. The corresponding chromophore structures associated with a particular state are illustrated in the inset of every SM-SERS spectra.

IV.3.2. Observing the 1510 cm⁻¹ peak in SM-SERS spectra

The time series SERS spectra of single GFP molecules under the employed experimental conditions are presented in Figure IV.5. The consecutive spectra at 100 ms intervals under 100 µW laser power indicate the GFP chromophore being captured in the A-state. According to the
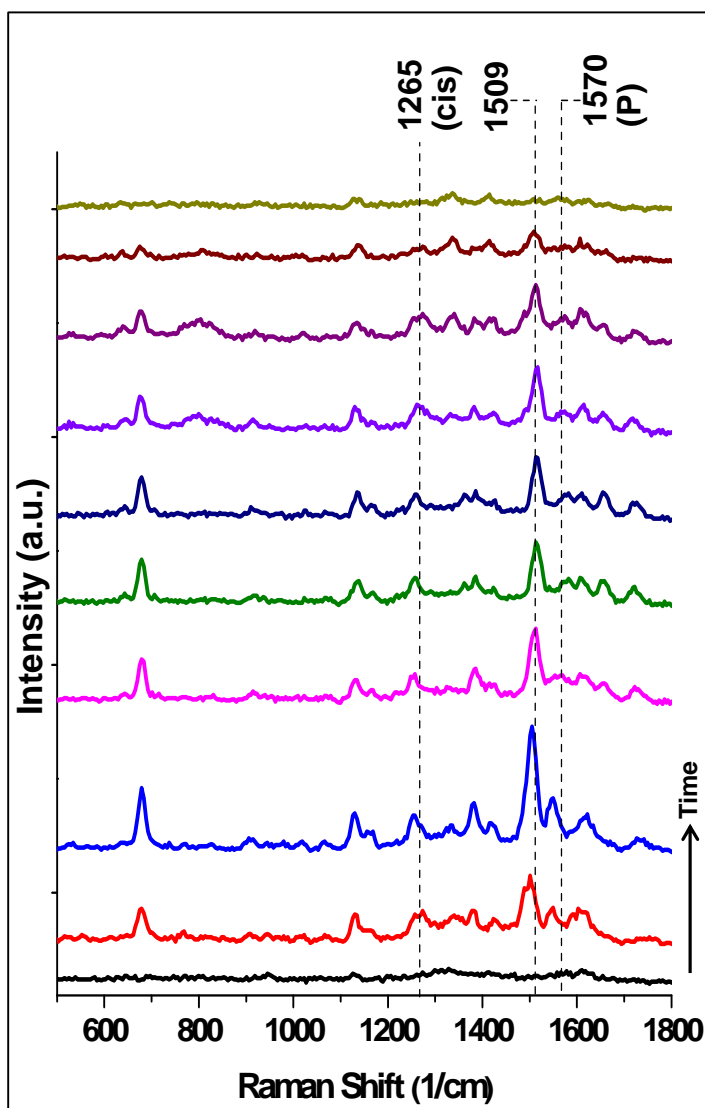
Figure IV.5. Time series SM-SERS spectra of a single GFP molecule captured employing the 405 nm LED external pump and 532 nm Raman probe. The 'spectral jump' demonstrates the appearance of a new peak at 1509 cm⁻¹ in addition to the adopted cis and protonated Raman markers. The consecutive SERS spectra are captured at an interval of 100 ms and under 100 µW laser power.

Raman markers adopted and summarized in Table IV.1, the cis and protonated Raman peaks at around 1265 cm^{-1} and 1570 cm^{-1} are observed, respectively. In addition, a new peak appears at around 1509 cm^{-1} and this is the first report that clearly demonstrates appearance of such a peak that dominantly accompanies the protonated (1260 cm^{-1}) Raman marker. However, this peak is consistently absent in SM-SERS spectra when the deprotonated Raman marker (1230 cm^{-1}) is observed. An example of this case is depicted in Figure IV.6. Here, appearance of both 1258 cm^{-1} and 1536 cm^{-1} peak indicate that the captured GFP chromophore is in the B-state. Typically, when GFP is captured at the B-state, the 1510 cm^{-1} peak is not observed. Application of 405 nm LED source as the pump and 532 nm as the Raman probe laser also yielded SM-SERS spectra capturing C and D-states of the GFP chromophore. But probability analysis of the captured states and peaks 1510 cm^{-1} peak concomitant with the A-state is significantly higher than those with other states. This point is discussed in detail in the later sections of this chapter.

Figure IV.7 shows the GFP chromophore in the C-state, as the 1286 cm^{-1} and 1565 cm^{-1} Raman markers for trans and deprotonation can be observed, respectively. Additionally, a peak at around 1505 cm^{-1} is also observed, which is similar to the SM-SERS spectra depicted in Figure IV.5. Though the chromophore is captured as cis and trans isomers in Figure IV.5 and Figure IV.7, respectively; their protonation state is same. This observation is particularly important as the new peak at around 1510 cm^{-1} can now be tether with a plausible relationship to the protonated form of the chromophore to gain a better insight on its' origin of appearance . Also it is now clear that, this Raman peak at ~1510 cm^{-1} can appear irrespective of the cis and trans conformations of the chromophore. But probability analysis indicates a higher chance of capturing this peak when the GFP chromophore is in its cis conformation.

Figure IV.6. Time series SM-SERS spectra of a single GFP molecule captured employing the 405 nm LED external pump and 532 nm Raman probe. The 'spectral jump' shows the cis and deprotonated Raman markers. The consecutive SERS spectra are captured at intervals of 100 ms and under 100 μW laser power.

Figure IV.7. Time series SM-SERS spectra of a single GFP molecules captured employing the 405 nm LED external pump and 532 nm Raman probe. The 'spectral jump' shows the trans and protonated Raman markers indicating chromophore is captured in the C-state. The consecutive SERS spectra are acquired at intervals of 100 ms and under 100 µW laser power.

Figure IV.8 illustrates a 'spectral jump' where a single GFP molecule is captured in the D-state. This can be confirmed as the Raman markers at around 1290 cm^{-1} and 1526 cm^{-1} indicate the chromophore to be in the trans and deprotonated conformation. A weak shoulder at around

Figure IV.8. Time series SM-SERS spectra of a single GFP molecule captured employing the 405 nm LED external pump and 532 nm Raman probe. The 'spectral jump' shows the trans and deprotonated Raman markers indicating chromophore is captured in the D-state. The absence of 1510 cm^{-1} peak is also noted. The consecutive SERS spectra are acquired at intervals of 100 ms and under 100 µW laser power.

1270 cm^{-1} indicates the cis Raman marker, which suggests that chromophore might have undergone a cis→trans transition during the 100 ms integration time. But the relative high intensity of the trans Raman peak indicate that the chromophore resided mostly in the trans-configuration during the integration period. Most importantly, the Raman peak at around 1510 cm^{-1} is not observed in this series of SM-SERS spectra. Thus, in summary it can be stated that this new and unique Raman peak (~1510 cm^{-1}) is observed to accompany both A and C states of the GFP chromophore. In comparison, this peak is substantially absent when the GFP chromophore is captured in both B and D states. So, the peak at around ~1510 cm^{-1} must have a direct relation with the protonation state of the chromophore. Monitoring this peak irrespective of cis and trans conformations of the chromophore indicate that this particular state of GFP chromophore can reside either in cis or trans configuration.

During a spectral jump, when a single GFP molecule is captured, as cis↔trans or/and protonation↔deprotonation transitions are observed once in a second on the average. Compared to an isolated molecule, which is capable of these transitions, this time scale of 1 s suggests a significant "slowing down" effect. This situation suggests that GFP chromophore is fairly stable in a particular state during the time of acquisition of the SM-SERS spectra, most likely due to stabilization by the β-barrel. Although the 1510 cm^{-1} peak is generally absent with the 1530 cm^{-1} Raman peak, some occurrences capture both of these peaks in the same 'spectral jump'. This can be considered rare under the employed experimental conditions. Figure IV.9 depicts such a rare occurrence that indicate the 1257 cm^{-1} (cis), 1508 cm^{-1} and 1536 cm^{-1} (DP) in the same 'spectral jump'. Both of the Raman peak at 1508 and 1536 cm^{-1} is observed in the spectra numbered 3 and 4. But in the subsequent spectra starting from 6 to 9 show only the 1508 cm^{-1} peak. During this period of acquiring SERS spectra, the GFP chromophore rests in cis- configuration. In particular, figure IV.9 indicates a rare probability of transitioning from one state to another one. Dominant

absence of co-appearance of these peaks also suggests that such a transition mostly likely

involves an inefficient process.

Figure IV.9. Time series SM-SERS spectra of single GFP molecules captured employing the 405 nm LED external pump and 532 nm Raman probe. The 'spectral jump' shows the cis and deprotonated Raman markers together with 1508 cm^{-1} peak. The consecutive SERS spectra are acquired at an interval of 100 ms and under 100 µW laser power.
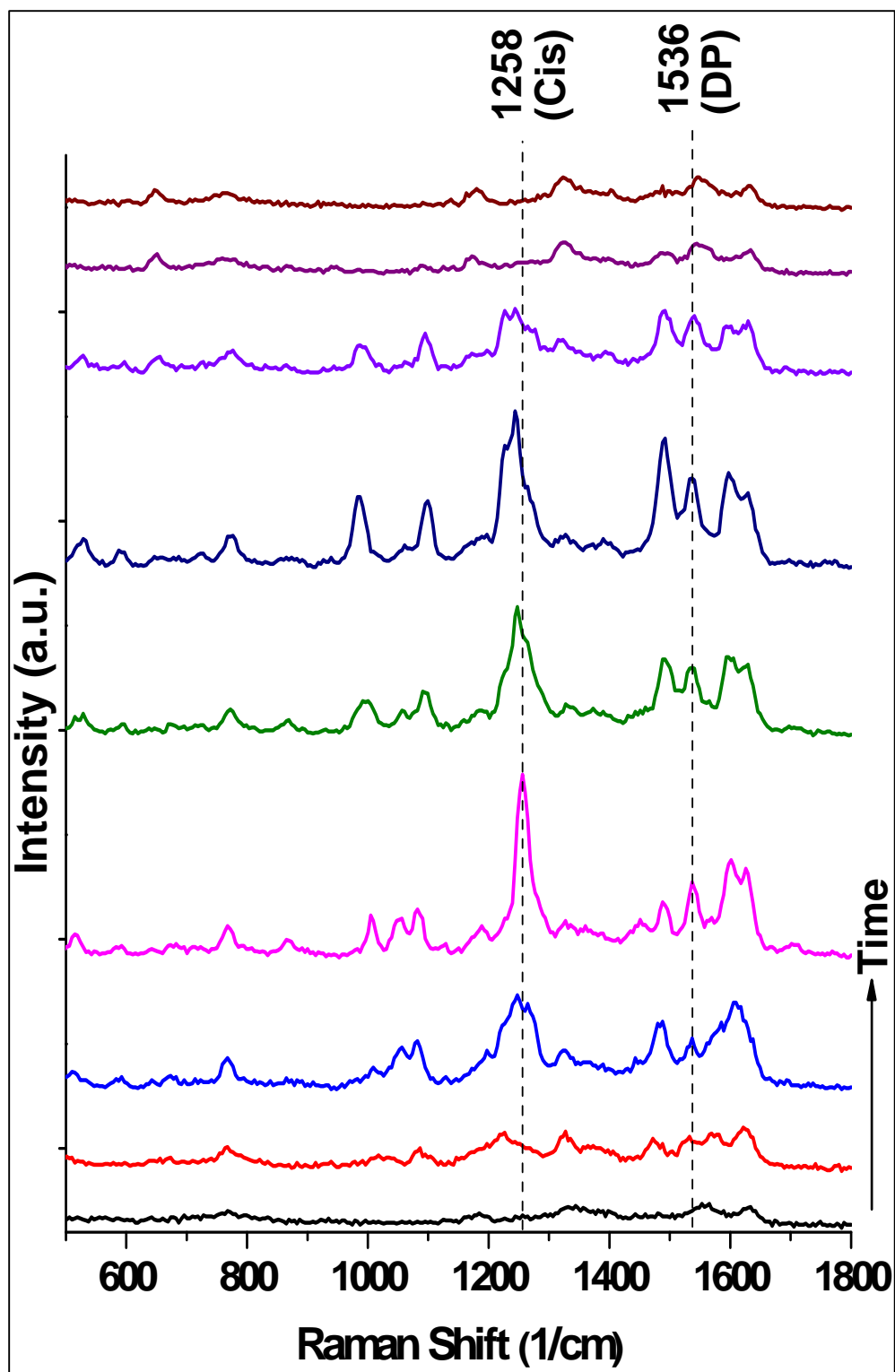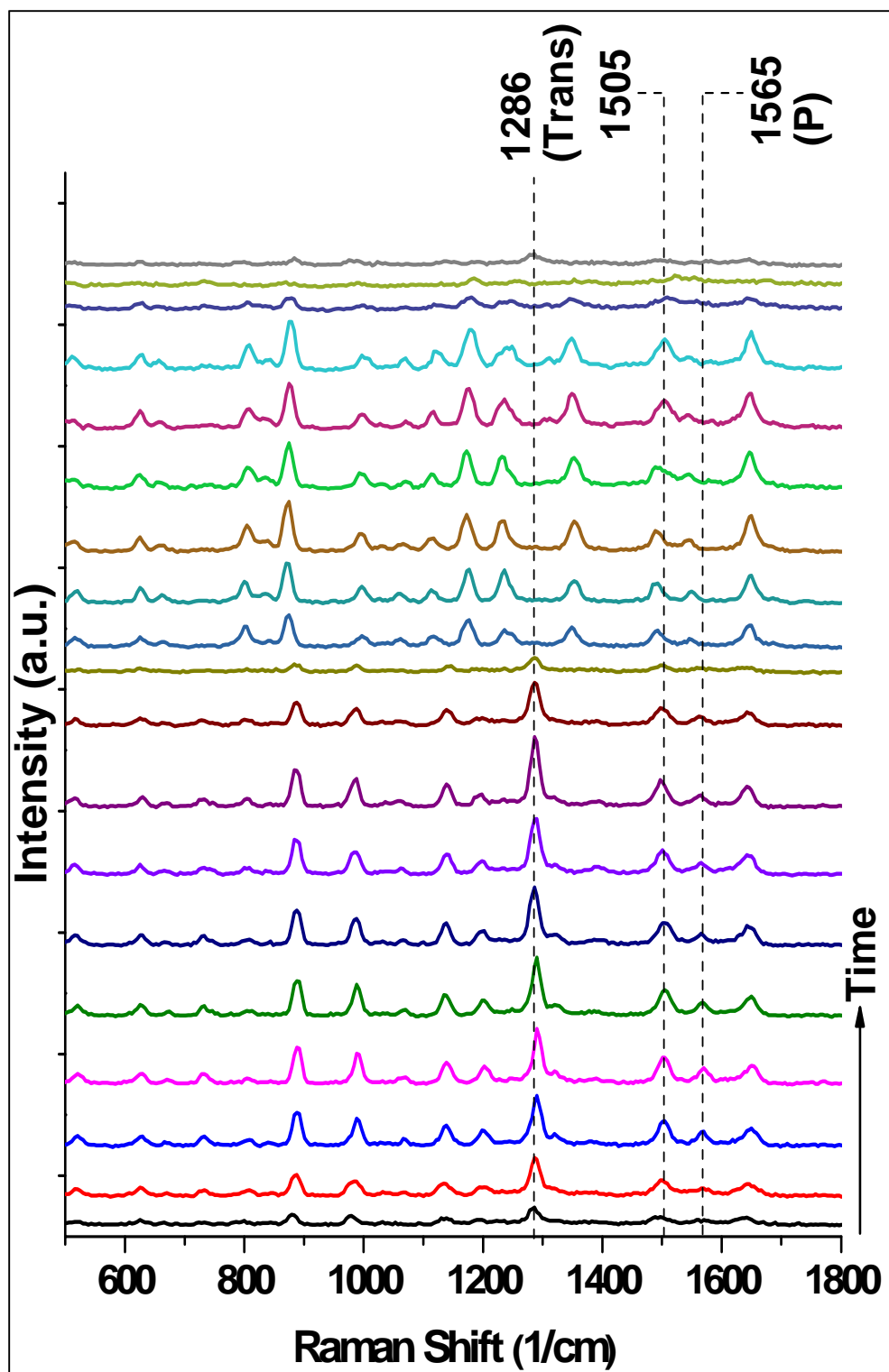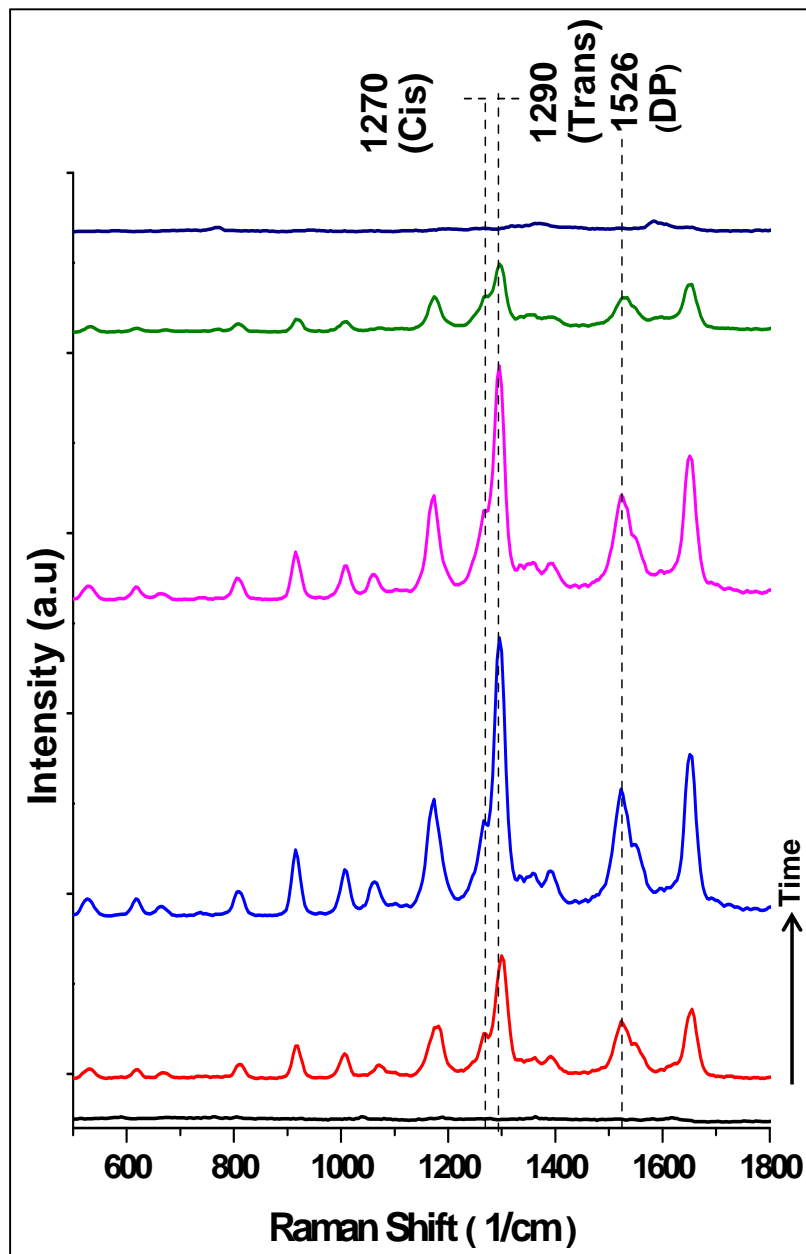
Figure IV.10. Time series SM-SERS spectra of a single GFP molecule captured employing the 405 nm LED external pump and 532 nm Raman probe. The 'spectral jump' shows the cis and protonated Raman markers together with 1505 cm^{-1} peak. The consecutive SERS spectra are acquired at intervals of 100 ms and under 100 μW laser power.

Some more evidences are presented before analyzing all the collected SM-SERS spectra. A conditional probability analysis of the GFP spectra is done and provided in the following section. However, Figure IV.10 displays a clear evidence of capturing both the 1505 and 1550 cm^{-1} peak in one 'spectral jump'. The GFP chromophore is captured in cis-configuration. This is another time evolution SERS spectra where GFP chromophore is captured in A-state. In this figure, both of these peaks appear at the same spectrum starting very early in the 'spectral jump'. 1505 cm^{-1} peak is observed to have relatively higher intensity than 1550 cm^{-1} (protonated) peak at the early stages of the SERS acquisition, but neither of the peaks completely disappears. This suggests that both of the peaks is associated with two different protonation states of the chromophore and belong to the "Förster cycle" of GFP. Figure IV.11 shows consistent appearance of the Raman peak at 1507 cm^{-1} together with 1564 cm^{-1} peak. In this 'spectral jump' both the peaks co-exist till the adsorbed single GFP molecule diffuses out of the 'hotspot'. GFP chromophore is observed in trans-configuration, identifying the C-state. Figure IV.11 also shows the absence of major structural transitions; which eventually leads to the aforementioned explanation of generating these two peaks from the "Förster cycle" of GFP under employed experimental conditions. Shifts between the peaks at 1505 and 1560 cm^{-1} can be observed, as displayed in the Figure IV.12, but appears to be very rare. In this figure, the peak at 1505 cm^{-1} shifts to the 1558 cm^{-1} peak as depicted in the spectra 5 and 6. The 1505 cm^{-1} peak disappears and only the 1558 cm^{-1} peak is observed for 3 more spectra before the reappearance of the 1505 cm^{-1} peak. The intensity of the peak at 1505 cm^{-1} gets higher before the SERS signal diminishes. A very crucial and important observation is that, and supported by the extensively collected SM-SERS spectra, the peak at 1505 cm^{-1} is not captured without the presence of the 1560 cm^{-1} (protonated) Raman peak. Such kind of occurrence is found to be extremely rare. This situation only verifies the explanation that both the peaks generate from the "Förster cycle" of GFP.

Figure IV.11. Time series SM-SERS spectra of single GFP molecules captured employing the 405 nm LED external pump and 532 nm Raman probe. The 'spectral jump' shows the trans and protonated Raman markers together with 1507 cm^{-1} peak. The chromophore is captured in C-state. The consecutive SERS spectra are acquired at an interval of 100 ms and under 100 µW laser power.

Also, observation of the protonated (1560 cm^{-1}) Raman marker is not dependent on observing the peak at 1505 cm^{-1} but the appearance of this peak is clearly dependent on observing the 1560 cm^{-1} peak. Thus 1505 cm^{-1} peak must belong to a photo-cycle (i.e. ""Förster cycle") that involves the protonated form of the chromophore excluded of the native deprotonated form (B-state). Figure IV.13 shows a 'spectral jump' without the appearance of the 1505 cm^{-1} peak together with 1533 cm^{-1} (DP). This is consistent with the above stated explanation that the 1505 cm^{-1} peak is not associated with the B-or D-state of the GFP chromophore.

Thus the key observations from the SM-SERS spectra of single GFP molecules employing 405 nm LED excitation as the pump and 532 nm as the Raman probe laser can be summarized in the following way:

(a) A new Raman peak at around 1505 cm^{-1} is prominently observed to appear with the protonated (1560 cm^{-1}) form of the GFP chromophore.

(b) This particular peak is observed to be significantly absent with the deprotonated (1530 cm^{-1}) form of the GFP chromophore.

(c) This peak is captured irrespective of cis and trans configuration of the chromophore, though cis- (1260 cm^{-1}) Raman marker is observed significantly more over trans (1280 cm^{-1}) Raman marker.

(d) Hence, this Raman peak accompanies mostly the A and C-states of the GFP chromophore. Very rarely it accompanies the B and D-states of the GFP chromophore. This suggests a highly probable association of this peak to the excited state photo-cycle of GFP involving either A or C state.
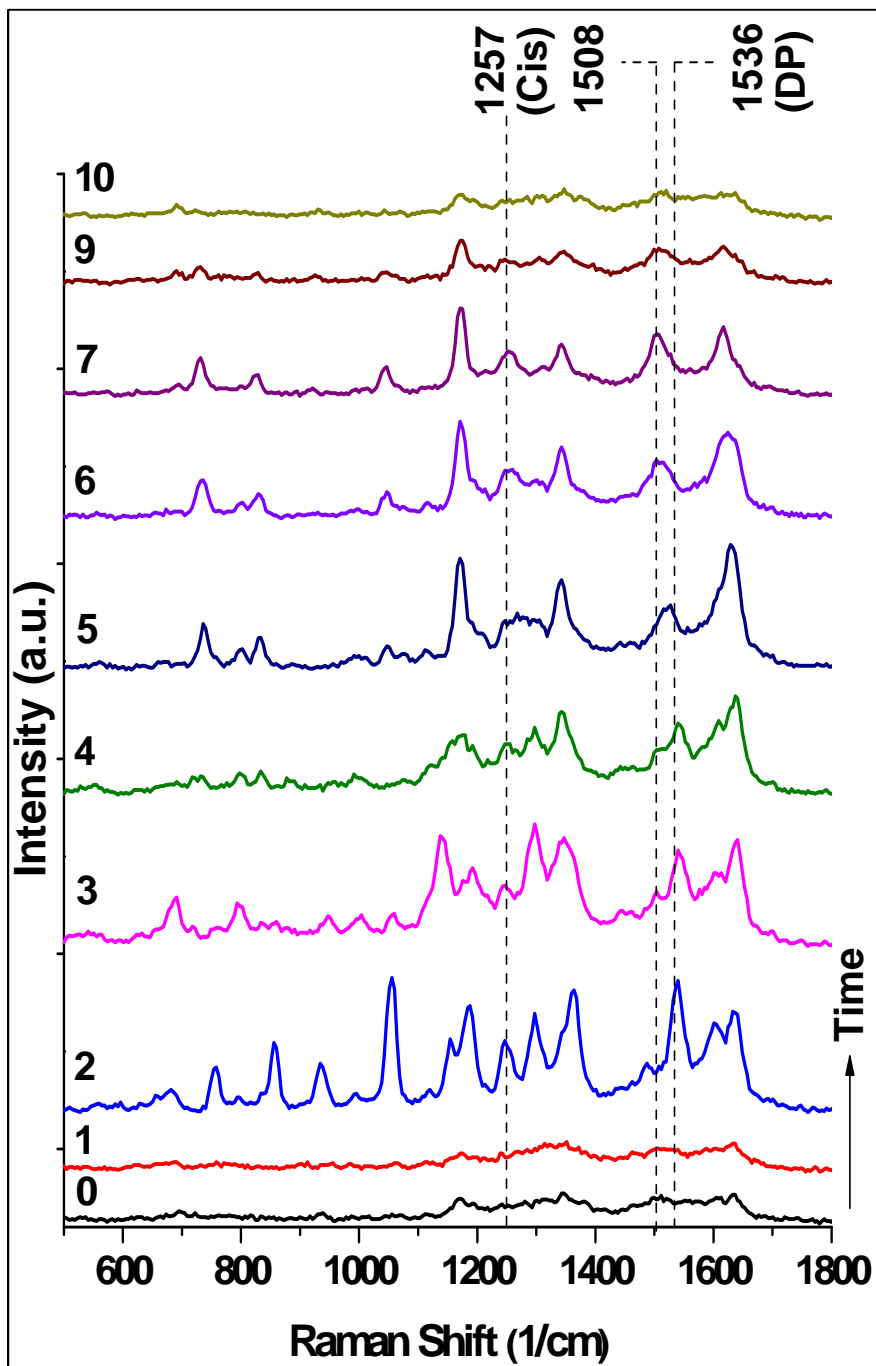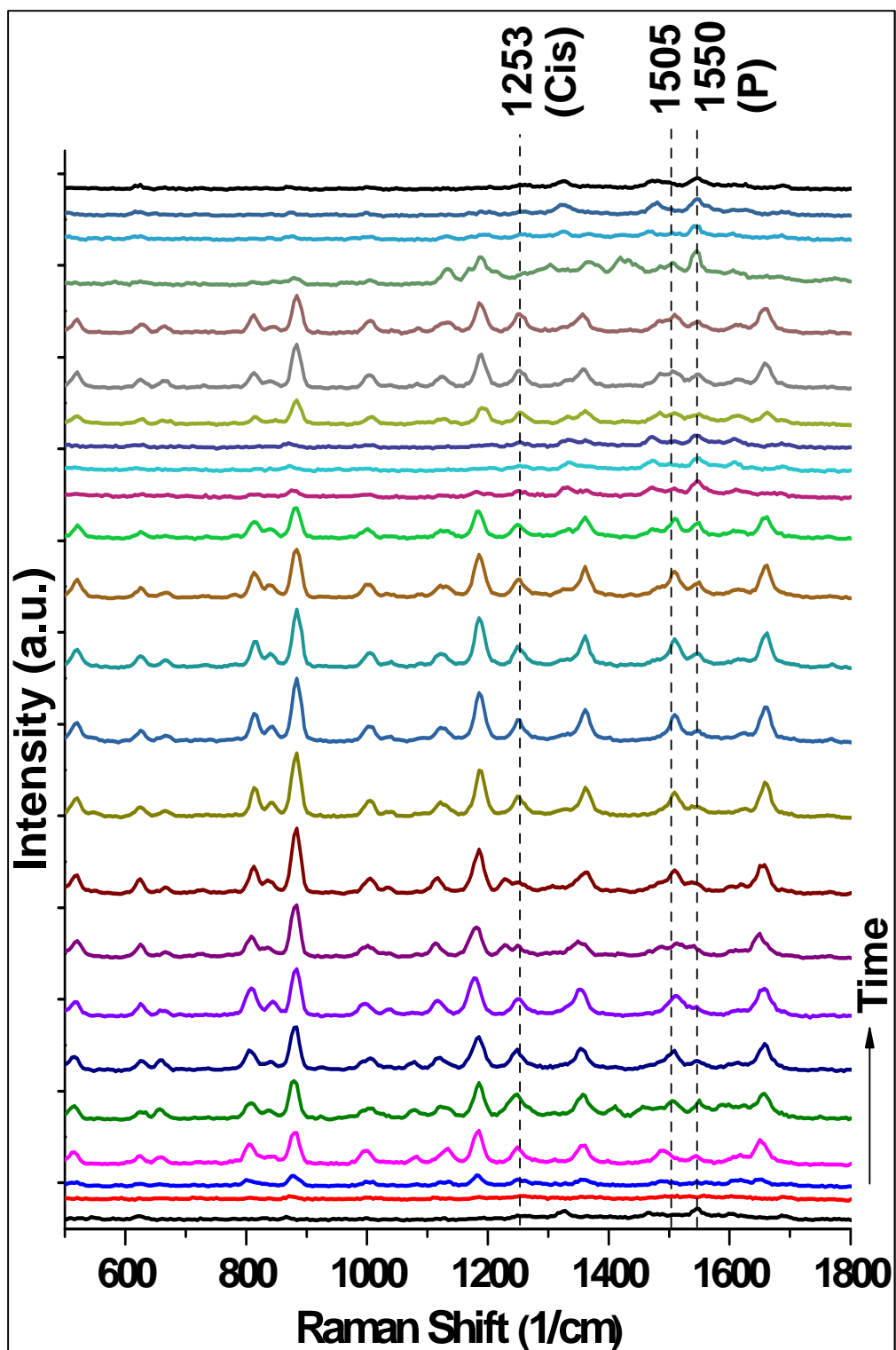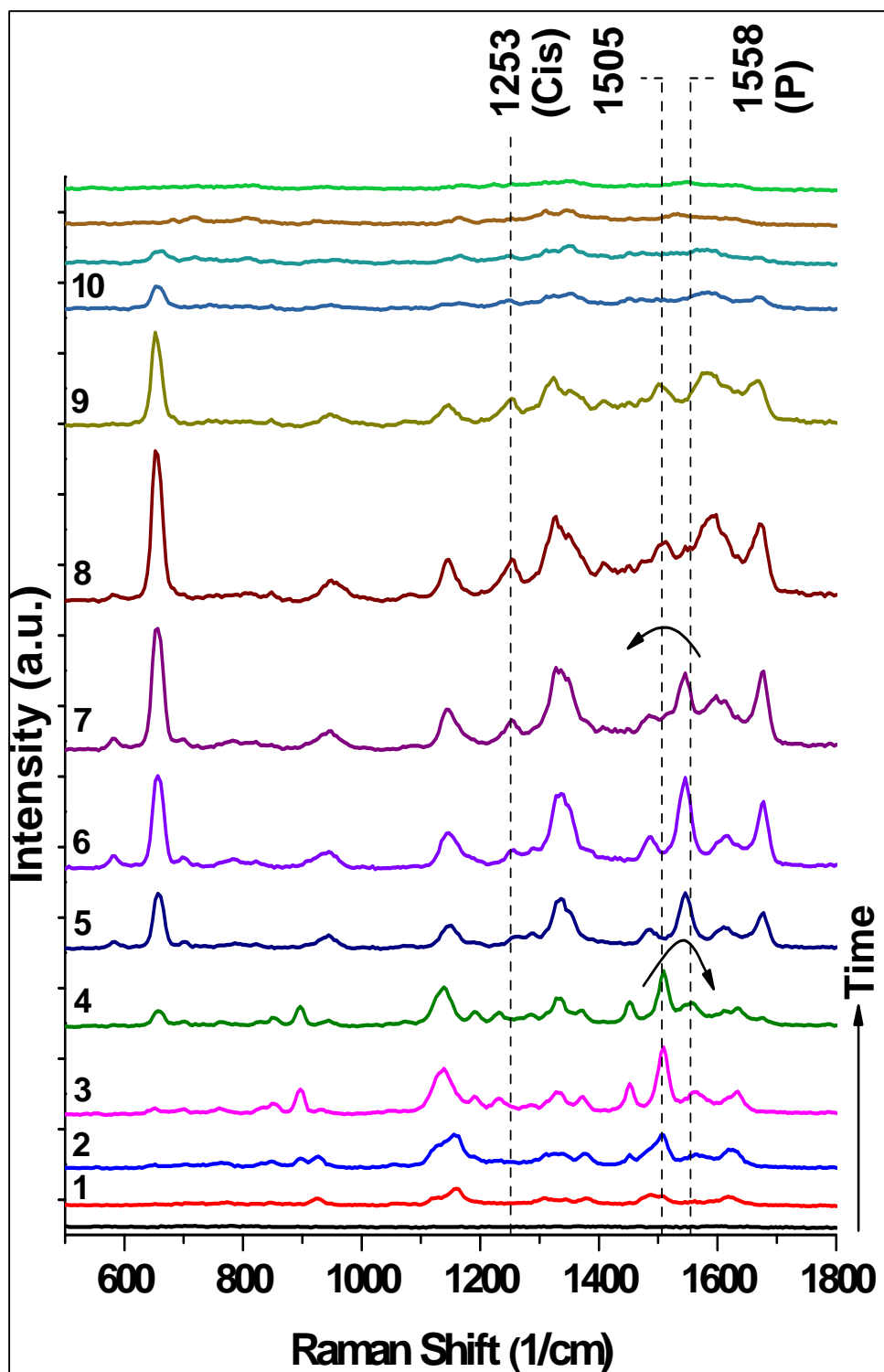
Figure IV.12. Time series SM-SERS spectra of a single GFP molecule captured employing the 405 nm LED external pump and 532 nm Raman probe. The 'spectral jump' shows the cis and protonated Raman markers together with 1505 cm^{-1} peak. Transition between 1505 and 1558 cm^{-1} is observed. The chromophore is captured in A-state. The consecutive SERS spectra are acquired at intervals of 100 ms and under 100 μW laser power.
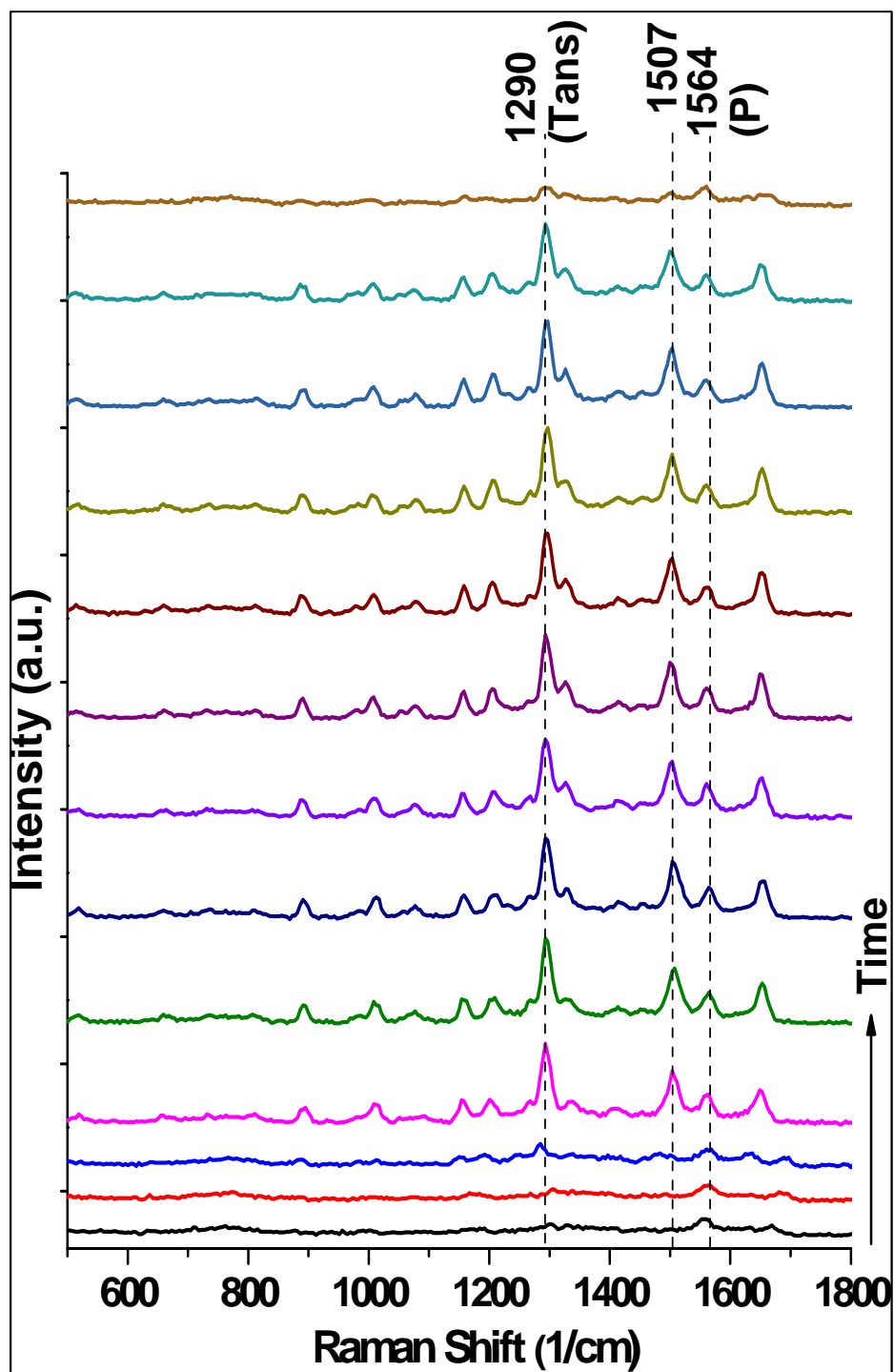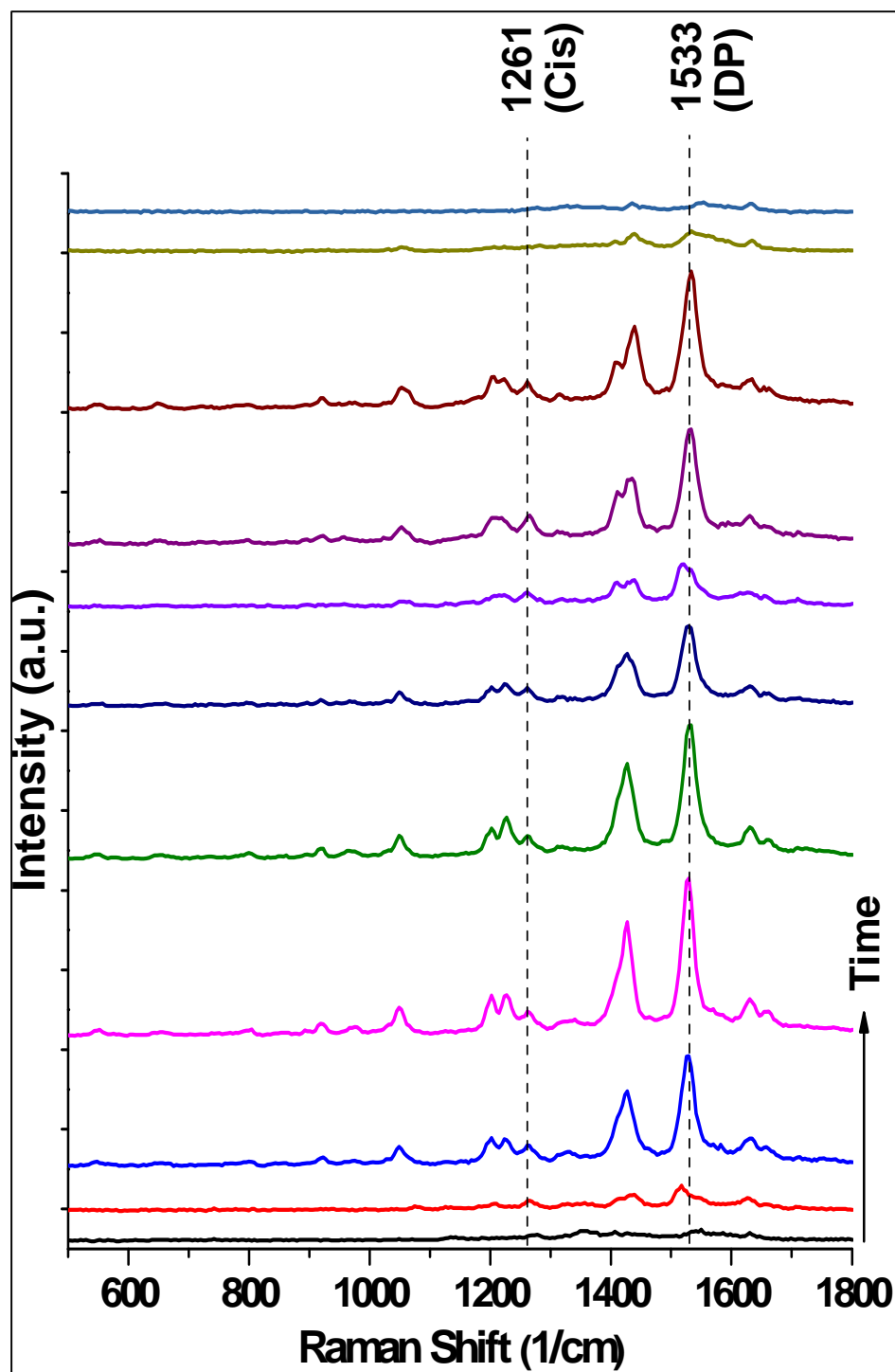
Figure IV.13. Time series SM-SERS spectra of a single GFP molecule captured employing the 405 nm LED external pump and 532 nm Raman probe. The 'spectral jump' shows the cis and deprotonated Raman markers in the absence of 1505 cm^{-1} peak. The chromophore is captured in B-state. The consecutive SERS spectra are acquired at intervals of 100 ms and under 100 µW laser power.

IV.3.3. Ascribing the 1510 cm^{-1} peak as the Raman marker for the 'intermediate (I) state' of GFP

Key observations together with the SM-SERS spectra have been presented in the previous section. It is stated earlier that the protonated form of the GFP chromophore is associated with the major absorption band (i.e. 395 nm) of the GFP population and can be directly excited by using an UV excitation source close to 395 nm. In turn, exciting the protonated form (A-state in the native GFP population) drives the 'Förster Cycle' and generates a unstable intermediate (I) state of the GFP chromophore, which quickly re-protonates to populate the ground state of the protonated (A-state) form of the chromophore. The 405 nm LED excitation (in addition to the excitation with 532 nm Raman probe laser) excites the native A-state (cis and protonated) of the GFP. Thus 'Förster cycle' (Figure II.4(b)) is driven and SERS signal is detected from single GFP molecules while fluorescence form the I-state is quenched due to GFP to nanoparticle energy transfer.

In general circumstances, it is highly improbable to capture Raman scattering from the unstable I-state of the GFP chromophore. In the 'Förster cycle'(Figure II.4(b)), the A-state is the stable form of the GFP chromophore and it rests in this A-state for a relatively longer period of time than the I-state. Thus most of the Raman signal is expected to be generated from this A-state of GFP. This situation is indeed true, as the protonated Raman maker is the only vibrational mode that had been captured and reported previously in all the Raman spectra.

On the other hand, a special circumstance is created in the present work due to surface-enhanced pumping (405 nm) by nanoparticles (Ag) that significantly reduces the inhabiting time of GFP in A-state. This in return can relatively increase the inhabiting time of I-state in the 'Förster cycle' to make it observable in the SM-SERS spectra. Also the Raman markers for the protonated and deprotonated forms of the GFP chromophore are 1560 and 1530 cm^{-1},

respectively; and associated with the stretching of the C=C double bond between the two rings (phenol and imidazolinone) of the chromophore. The vibrational mode frequency is lowered with deprotonation of the phenolic oxygen. Figure II.3 indicates the unstable I-form of the chromophore with less hydrogen bonding (H-bond) than the B-state. Thus, it is expected that I-state is associated with a further shift towards lower frequency than the B-state. Based upon these considerations, it is hypothesized that the 1510 cm^{-1} ($\pm 5 \text{ cm}^{-1}$) peak is the Raman marker for the I-state of the GFP chromophore. The following section will provide a theoretical analysis to develop a framework of arguments to validate the possibility of capturing the I-state of GFP by SM-SERS.

IV.4. Theoretical analysis to validate the assignment of 1510 cm^{-1} peak to the I-state Raman marker

It is well established in the literature that the I-state, associated with the 'Förster cycle' of the GFP (Figure II.4 (b)), is an unstable state at room temperature. As mentioned in the Figure II.4 (b), the lifetime of the I-state is 400 ps due to quick re-protonation to form the A-state (I→A). The 'Förster cycle' (Figure II.4 (b)) involves recurring deprotonation and protonation of the chromophore. Interconversion as a cycle between the ground and excited states of A and I form of the chromophore (A→A*→I*→I→A) is efficiently driven under UV excitation. The fraction of the time chromophore inhabits in I-state can be given by, $X_I = \frac{\tau_I}{\tau_A + \tau_{A^*} + \tau_{I^*} + \tau_I}$. Here all the **'τ'** represents the corresponding lifetimes of the states. From the Figure II.4 (b), all the lifetimes of the states associated with the 'Förster cycle' can be known except the lifetime of the A-state. The lifetime of A-state, τ_A, depends on the optical pumping rate for a molecule (in power) and can be expressed in the form of the following equation:

$$P = I_{405\ nm} \times \sigma = n \times E_{photon} = \frac{\hbar\omega}{\tau_A} \quad (1)$$

Here, $I_{405\ nm}$ is the incident intensity of the excitation light, σ is the absorption cross-section of wtGFP in A-state ($\sim 10^{-16}$ cm^2), n is the number of absorbed photon per unit time and $\hbar\omega$ is the photon energy. If 1 mW incident power (typical for fluorescence spectroscopic measurements) and diffraction limited focused spot size of 1 μm is considered for 405 nm then $I_{405\ nm}$ is about $10^5\ W/cm^2$ according to the following calculation.

$$I_{405\ nm} = \frac{10^{-3}W}{10^{-8}cm^2} = 10^5\ W/cm^2$$

Accordingly, putting the values of Planck constant (6.63×10^{-34} J.s), velocity of light (3×10^8 m/s) and wavelength of incident light (405 nm) in equation (1) τ_A is found to be in the order of 50 ns.

$$10^5\ \frac{W}{cm^2} \times 10^{-16} cm^2 = \frac{\hbar\omega_{405\ nm}}{\tau_A}$$

$$10^{-11}W = \frac{(\frac{6.63 \times 10^{-34}\ J.s\ \times 3\ \times 10^8\ ms^{-1}}{405 \times 10^{-9}\ m})}{\tau_A}$$

Thus we can safely assume that the fraction of time GFP resides in state A, τ_A, is in the order of maximum 100 ns. And X_I is computer to be less than 0.004 according to the following equation,

$$X_I = \frac{400\ ps}{100\ ns + 8\ ps + 3\ ns + 400\ ps}$$

It is obvious from the poor time-averaged intensity of the I-state of the GFP chromophore that it cannot be observed under the above mentioned conditions using conventional spectroscopic techniques. The fraction of time GFP resides in A-state is the limiting factor that is responsible for the poor time averaged signal of the I-form. Thus reduction of τ_A as well as τ_{I^*} will relatively increase the fraction of time GFP inhabits the I-state.

The X_I can be enhanced dramatically under a favorable combination of effects. First, τ_A is expected to be shortened by the near field enhancement of optical pumping by the Ag nanoparticles. Dramatic enhancement of excitation is reported by Malicka *et al.* when Cy3 fluorophore is attached in close proximity (100 Å) to the silver island films (SIF) [82]. The increase in fluorescence is also associated with the decrease in lifetime and according to Malicka *et al.* 3 orders of magnitude excitation enhancement can be achieved [71, 82-84] Also the decay lifetime is reported to shorten by 25-fold due to the presence of silver [82]. If similar magnitudes are considered in shortening the lifetimes associated with A and I* states, then τ_A and τ_{I^*} roughly shortens to ~100 and ~120 ps, respectively and as a consequence, X_I can reach ~0.65. But the particular SERS substrates used in these experiments can achieve a SERS enhancement factor of 10^{10} enabling single molecule detection. Thus the enhancement in optical pumping due to Ag nanoparticles can be expected to reach ~10^5. In such a case, X_I can reach ~0.8 and can even approach unity with further enhancement.

This above discussed analysis suggests that the high intensity of the 405 nm radiation is a critical precursor to effectively photo-generate the I-state population. It is believed that such favorable conditions are achieved for most of the part due to the surface-enhanced pumping. Overall, shortening of the inhabiting time of GFP chromophore in A-state and further shortening of the emission time of I* state, can increase the relative inhabiting time of the chromophore in the I-state. Thus increase in population (or inhabiting time in single molecule case) of the I-state facilitates its appearance during the acquisition of Raman spectra. A general concern may raise the question on the possibility of photo-degradation (i.e. photo-bleaching) of GFP molecules under such high intensity radiation. But, this concern is solved due to the decreased lifetime (τ_{I^*}) of the excited intermediate state, I*, which will allow GFP to undergo more excitation-deexcitation cycles before eventual photochemical degradation [85].

IV.5. Statistical analysis of the captured GFP states

Extensive statistical analysis (a total of 712 SM-SERS spectra collected from 64 'spectral jumps') has been carried out to validate the hypothesis that the observed 1510 cm^{-1} ($\pm$5cm^{-1}) peak is the Raman marker for I-state of the GFP chromophore associated with the 'Förster cycle'. I state is unstable as well a very dynamic component in the 'Förster cycle'. In general, the frequency of this I-state can reach 1 MHz as discussed in the section IV.3. The cycle frequency of I-state can increase due to enhanced optical pumping by nanoparticles and can reach ~10^5 or more cycles between the states A and I during a SERS integration time of 100 ms. As a result, the SERS signal from both the states are integrated. Thus it expected that the Raman peak around 1510 cm^{-1} will appear together with the A-state Raman markers at 1260 and 1560 cm^{-1}. Such occurrences are consistently observed under the employed experimental conditions in this present work. The probability histogram presented in Figure IV.14 (a) validates such condition. Figure IV.14 (a) presents conditional probabilities of different conformational states to justify the hypothesized correlations. Probability of observing a given conformational Raman marker with respect to the other markers is plotted. It is observed from Figure IV.14 (b) that for a given single molecule SERS spectrum including the hypothesized I-state marker (1510 cm^{-1}), the probability of observing the protonated (P, 1560 cm^{-1}) Raman marker is about 88%. As the I-state marker is a component associated only with the 'Förster cycle', the 1510 cm^{-1} peak must be exclusive with the deprotonated (DP, 1530 cm^{-1}) Raman marker. This fact is also observed to be consistent with our hypothesis as the correlation between the 1510 and 1530 cm^{-1} peak is found to be merely 9% as provided in Figure IV.14 (b).

The native A-state of the GFP chromophore resides in cis and protonated configuration. Thus the I-state being the deprotonated form of the A-state should also reside in cis configuration. Hence, cis marker (1260 cm^{-1}) should also accompany the 1510 cm^{-1} peak in a SM-SERS spectrum. This kind of correlation of observing cis marker given the I-state marker is found to be

about 70%, which is less than the correlation between I and P Raman markers (i.e. 88%). But interestingly, trans marker ($1280 cm^{-1}$) also indicates a correlation of 39% with the $1510 cm^{-1}$ peak (Figure IV.14 (b)). This indicates that I-form of the chromophore can also reside in trans-configuration, though with a lesser population than that of cis-configuration. Interestingly, this finding suggests the "Förster cycle" can also undergo as C→C*→I*→I→C. A correlation of about 20% (Figure IV.14 (b)) is observed for trans→cis type of transition (isomerization). This suggests that trans→cis type of isomerization occurs in every 500 ms on the average. Such a rate of transition is significant and indicates that photoisomerization is induced as the 405 nm pump resonantly excites the A and C-states of GFP.

Excitation of the A and C-states (protonated) is achieved by 405 nm LED source. Hence, a strong correlation is expected between the $1510 cm^{-1}$ peak and A-and C-states of GFP (Table IV.1). Indeed, a strong correlation of 97% is observed as presented in Figure IV.15 (b). Again, correlation of 36% is also observed and presented in figure IV.15 (a), (b) between the C (trans and protonated) and I-state ($1510 cm^{-1}$) of GFP, implying the possibility of 'Förster cycle' occurring between I and C.

Similarly, given A or given C, the probability of observing I is also high. The probability of observing $1510 cm^{-1}$ (I-state) peak given that the GFP chromophore is in the A-state is 87%, while a correlation of 80% is found for observing I-state peak given C-state as presented in Figure IV.15 (b). Both of these correlations strongly agree with the explanation that "Förster cycle" is detected and $1510 cm^{-1}$ peak is the I-state marker of GFP.

(a)

(b)

Given\Corr.	Cis	Trans	P	DP	I
Cis	-	19.14	64.81	74.65	69.63
Trans	9.12	-	41.65	35.21	38.87
P	67.22	90.62	-	31.92	87.62
DP	29.61	29.29	12.21	-	9.09
I	67.03	78.51	81.33	22.06	-
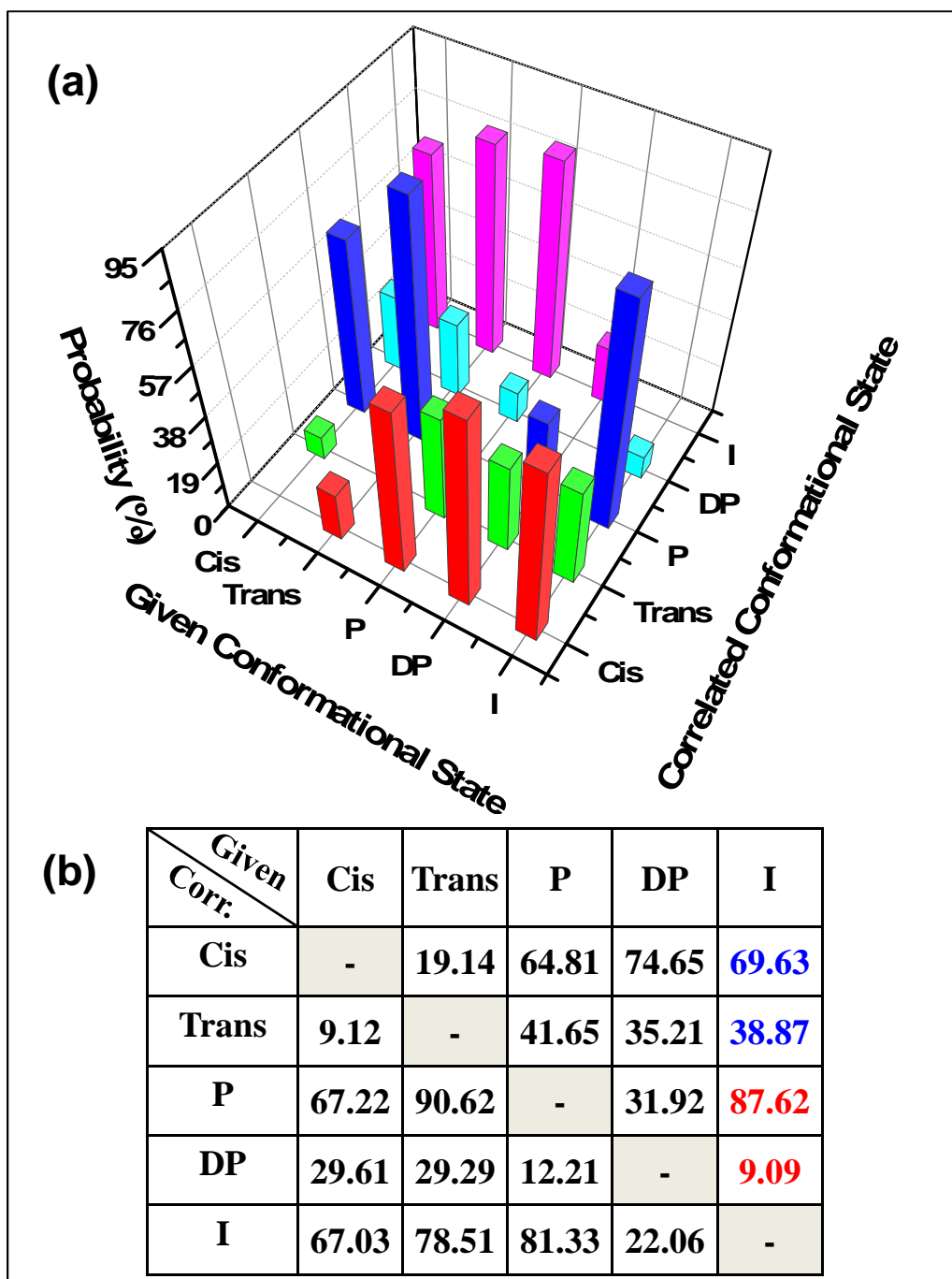
Figure IV.14. (a) Probability of capturing different conformation (cis, trans, protonated, deprotonated, intermediate) of GFP chromophore for a given conformation. (b) Statistical analysis of the GFP conformations based on 712 single molecule spectra collected from 64 'spectral jumps'.

(a)

(b)

Given \ Corr.	A	B	C	D	I
A	-	13.84	15.52	20	**61.12**
B	6.09	-	6.46	30.67	**7.35**
C	9.97	9.43	-	80	**35.97**
D	4.15	14.46	25.86	-	**5.41**
I	87.53	23.9	80.17	37.33	-
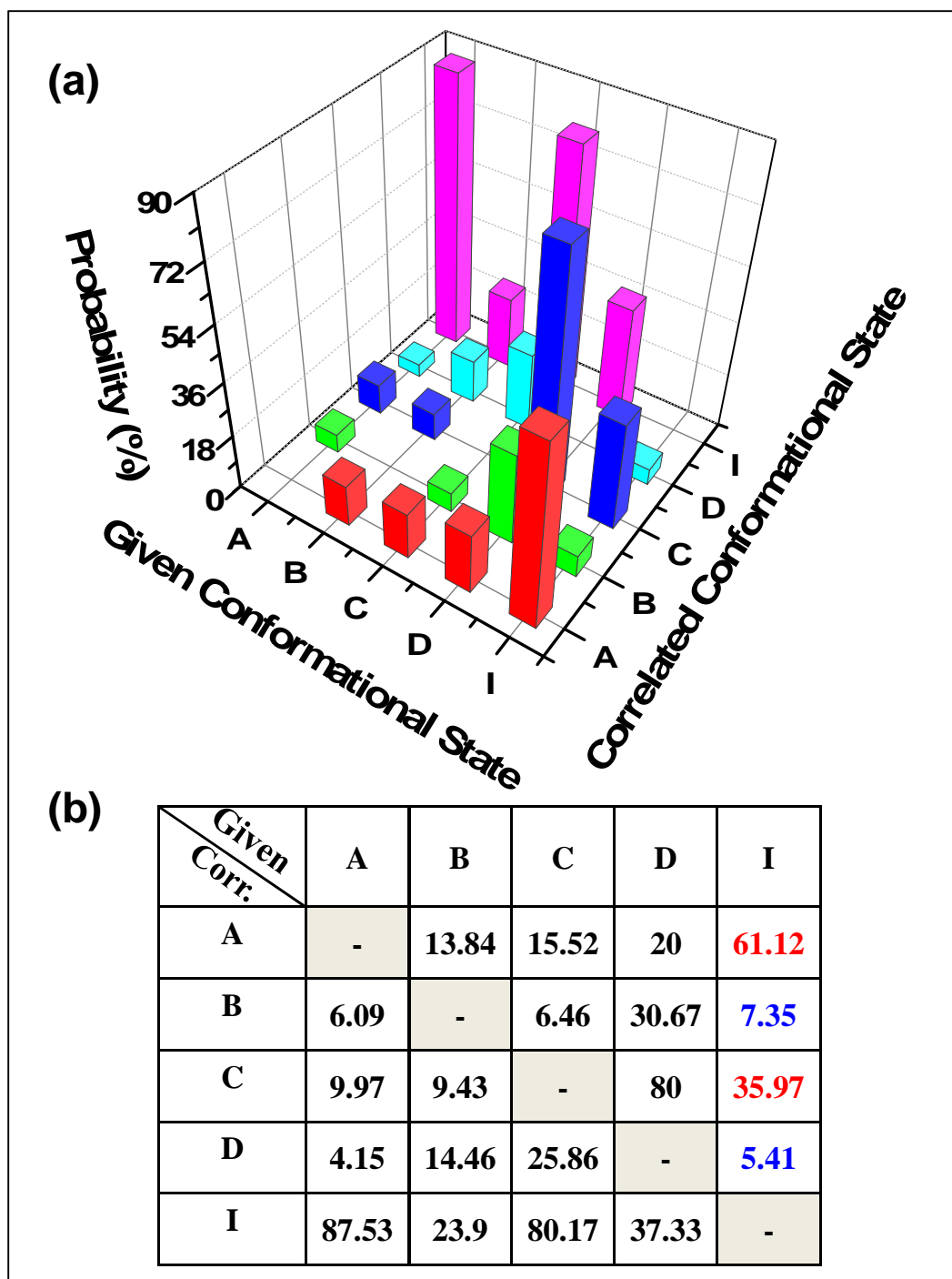
Figure IV.15. (a) Conditional probability diagram showing correlations between different (A, B, C, D, I) states of GFP chromophore. (b) Statistical analysis of the different states of GFP population based on 712 single molecule spectra collected from 64 'spectral jumps'.

As mentioned earlier, the fraction of time I-state spends in the "Förster cycle" must have

to increase with nanoparticle-enhanced optical pumping or equivalently with the surface-

enhancement factor. Accordingly, the fraction of time chromophore resides in the A-state of the

"Förster cycle" will also decrease. This suggests that, the ratio of the intensity of I state

(Intensity $_{1510}$) marker to that of A-state (Intensity $_{1560}$) marker (i.e. $\frac{Intesity_{1510}}{Intesity_{1560}}$) must indicate a

positive slope. Hence, to validate this explanation, the intensity of 1510 (I-state marker) and 1560

cm^{-1} (protonated marker) is counted from every SM-SERS spectrum that captured either of the

two marker peaks. Then the ratio of these two peaks (i.e. $\frac{Intesity_{1510}}{Intesity_{1560}}$) is plotted against

Intensity$_{1560}$. A simple relationship to check the fit of the plotted data is also derived in the

following way:

Fraction of time "Förster cycle" resides in I-state, $X_I = \frac{\tau_I}{\tau_A + \tau_{A^*} + \tau_{I^*} + \tau_I}$ (2)

From Figure II.5. (b), the inhabiting time (τ) of every state is known excluding τ_A. Assuming

other life times (i.e. inhabiting time) to remain constant, $C = \tau_{A^*} + \tau_{I^*} + \tau_I$ and $\tau_I = A$ can be

substituted. Then, simplified eq. (2) becomes,

$$X_I = \frac{A}{\tau_A + C}$$

The electromagnetic field, E acting on the states is considered to be proportional to the square of

the surface enhancement factor, G; i.e. $E \propto G^2$. The overall enhancement of the electromagnetic

field is considered to be $E^4 \propto (G_{SERS}^2 G_{Raman}^2)$ [25].

Accordingly, inhabiting time of A-state, τ_A can be found in the following way,

$$\tau_A \propto (\frac{Constant}{E}) \propto (\frac{Constant}{G^2})$$

$$\tau_A = \frac{B}{G^2}$$

Putting the value of τ_A in eq. (2),

$$X_I = \frac{A}{\frac{B}{G^2} + C}$$

To simplify the above equation we can neglect C, as $C \ll 1$ ($\tau_{A^*} = 8 \, ps, \tau_{I^*} = 120 \, ps, \tau_I = 400 \, ps$) and accordingly X_I becomes,

$$X_I = \frac{A}{B} G^2$$

Again, fraction of time "Förster cycle" resides in A-state, $X_A = \frac{\tau_A}{\tau_A + \tau_{A^*} + \tau_{I^*} + \tau_I}$

Putting the value of τ_A and $\tau_{A^*} + \tau_{I^*} + \tau_I = C$, X_A becomes,

$$X_A = \frac{\frac{B}{G^2}}{\frac{B}{G^2} + C}$$

To simplify the above equation we can also neglect C, as $C \ll 1$ and accordingly X_A becomes,

$$X_A \cong 1$$

Then, intensity of I-state, $I_{1510} \propto (X_I \times E) \propto (X_I \times G^4)$ and intensity of A-state, $I_{1560} \propto (X_I \times E) \propto (X_A \times G^4)$ .The ratio of these two intensities,

$$\frac{I_{1510}}{I_{1560}} \propto \left(\frac{X_I}{X_A}\right) \propto \left(\frac{A}{B} G^2\right)$$

On the other hand, intensity of A-state becomes, $I_{1560} \propto (X_A \times G^4) \propto (G^4)$

Thus, if $\frac{I_{1510}}{I_{1560}}$ is plotted in the y-axis and I_{1560} is plotted in the x-axis, a simple relation as the following one can be derived,

$$y = \left(\frac{A}{B}\right) \times \sqrt{x}$$

Accordingly, a plot of $\frac{I_{1510}}{I_{1560}}$ vs I_{1560} should show a relationship of the kind, y $\propto (x)^{\frac{1}{2}}$.

Such a relationship could not be verified in this thesis work because two different excitation sources (i.e. 405 and 532 nm) are used in the experiments. The above mentioned relationship between the intensities of the 1510 and 1560 cm^{-1} peak is derived by considering only a single 405 nm excitation source and thus cannot be implemented under current experimental conditions. But this derivation is useful as a theoretical framework to validate the existence of such a relationship if a single source of excitation (i.e. 405 nm as both the pump and the Raman laser probe) is used in the future.

Interestingly, if I_{1560} ($y - axis$) is plotted against. I_{1510} ($x - axis$) (Figure IV.16) then a monotonous relationship is observed. Most of the data points (both state A and state C) fall in a region where intensities of both the 1510 and 1560 cm^{-1} peak are comparable. This suggests that the 'hotspots' act both as a good Raman and 'Förster cycle' pump. That means, the 'hotspots' have significant nanoparticle-enhanced optical pumping in addition to the high SERS enhancement to facilitate integration of comparable signals (intensities) from both the 1510 and 1560 cm^{-1} peaks. However, few 'hotspots' can have high SERS enhancement but not a significant

nanoparticle-enhanced optical pumping. In such cases, significant high intensity of the 1560 cm^{-1} peak is observed compared to the intensity of the 1510 cm^{-1} peak.
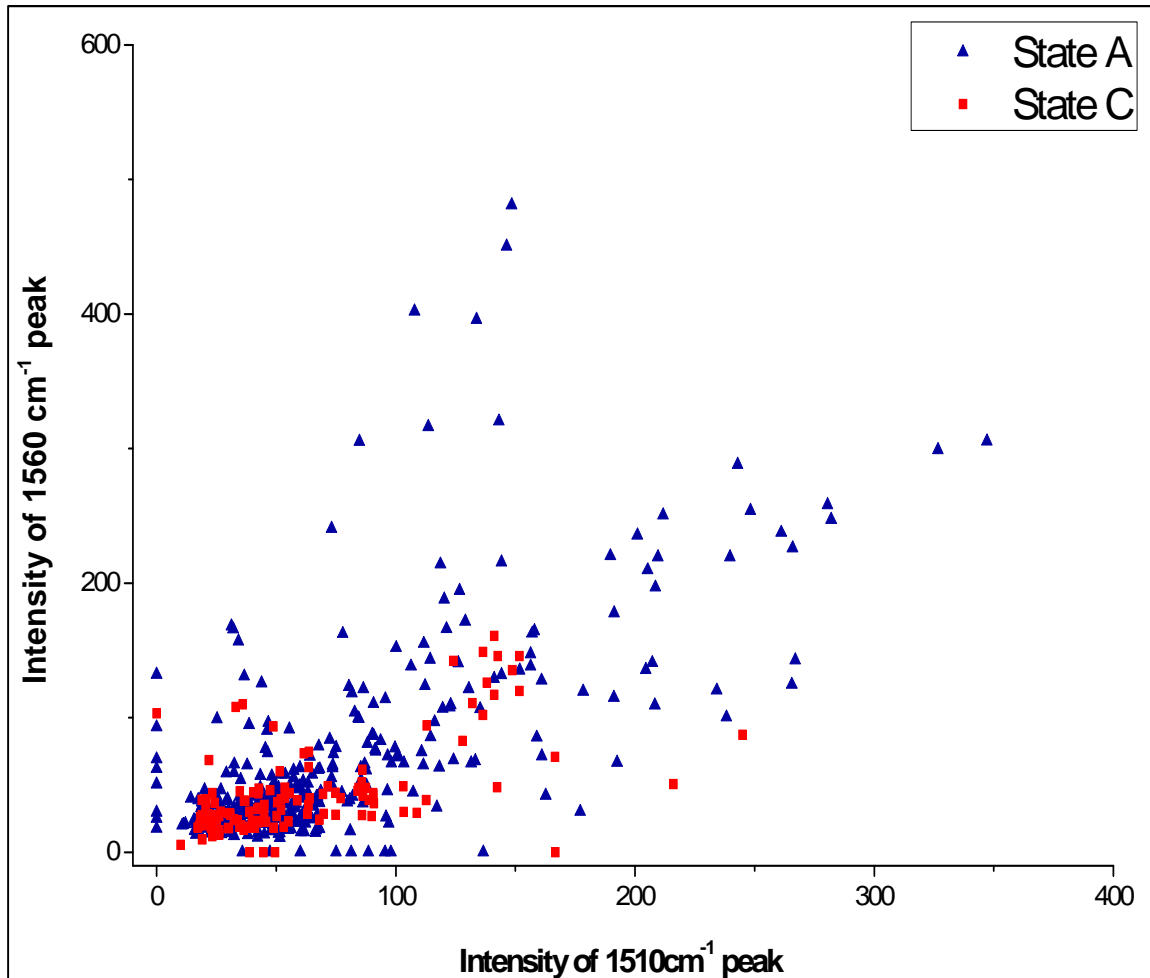
Figure IV.16. Intensity of 1560 cm^{-1} peak against the intensity of 1510 cm^{-1} peak as plotted for both the A and C-states of GFP.

CHAPTER V

CONCLUSIONS

The present thesis work employs novel 'nanometal-on-semiconductor' SERS substrates developed by Kalkan *et al.* [21, 22, 24] to acquire Raman spectra of single wtGFP molecules. 405 nm LED source is used as the pump to excite the native cis and protonated (A-state) form of the GFP chromophore, while 532 nm is employed as the Raman probe laser. SERS acquisitions result in repeated observation of appearance and disappearance of strong and clearly resolvable peaks over a weak background after spotting an aliquot of 1×10^{-9} M wtGFP solution on the SERS substrate. These temporal "spectral jumps" captured in every half a minute on the average are associated with single GFP molecules diffusing in and out of enhancement factor SERS sites (i.e. "hotspot") with an average residing time of 1s or less. SERS is acquired as a continuous time series spectra at intervals of 100 ms. On the average about 15 single molecule spectra can be captured during a "spectral jump". The following pivotal conclusions are drawn and summarized based on the results discussed in this thesis.

1. The analysis of the time series SERS spectra shows consistent appearance of a new Raman peak at around 1510 cm^{-1} under the employed experimental conditions. This 1510 cm^{-1} peak is not observed in the absence of 405 nm radiation. This unique Raman

63

peak co-exists with the protonated Raman marker (1560 cm^{-1}) of the GFP chromophore. This peak has never been reported to appear. Also significant absence of this peak is observed in the single molecule spectra of GFP with deprotonated Raman marker (1530 cm^{-1}).

2. Considering continuous excitation of the native A-state (cis and protonated) of the GFP chromophore by the 405 nm pump and dominant co-existence of the protonated peak with significant absence of the deprotonated peak with this new peak (1510 cm^{-1}) suggests it is associated with the I-state of the "Förster cycle" of GFP i.e. A→A*→I*→I→A. Each SM-SERS spectrum is a collective snapshot of the interconverting states involved in the photodynamics of the "Förster cycle" integrated over the time interval (100 ms) to reveal dominantly residing states in a photo-cycle. This never before reported Raman peak at around 1510 cm^{-1} is thus associated with a dominant state involved in the "Förster cycle". As reported earlier, the 1560 and 1530 cm^{-1} Raman peaks are the markers for the protonated and deprotonated form of the GFP chromophore, respectively; and are associated with the C=C double bond stretch bridging the phenol and imidazolinone rings. It is observed that, the vibrational mode frequency is lowered with the deprotonation of the phenolic oxygen. Intermediate (I) form, a key state in the "Förster cycle" of the chromophore, is an un-relaxed form of the B-state (cis and deprotonated) with less hydrogen bond stabilization around the phenolic oxygen. Thus a further shift towards the lower mode frequency can be attributed to the I-state of the GFP. Therefore, 1510 cm^{-1} peak is identified as a unique Raman marker for the I-state of the GFP chromophore and also as a maker to confirm the detection of the "Förster cycle" at the single molecule level.

3. Statistical analysis of the captured SERS spectra of single GFP molecule indicates a dominant appearance of this I-state marker at around 1510 cm^{-1} with the protonated (P) Raman peak at 1560 cm^{-1}. It is observed from the conditional probability analysis of the GFP conformational states: A(cis/protonated), B(cis/deprotonated), C(trans/protonated) and D(trans/deprotonated);

that for a given single molecule SERS spectrum that includes the I-state marker, the occurrence of the protonated Raman marker is about 88%. This is more than 9 times than the probability of capturing both the I-state and deprotonated Raman peak in a SERS spectrum of single GFP molecules. The probability of capturing the deprotonated peak, 1530 cm^{-1}, given that the I-state peak is also observed in the same SERS spectrum is only about 9%. I-state is the deprotonated form of the A-state and should be in the cis-configuration as the native A-state. Interestingly, this correlation of observing the cis Raman marker, 1260 cm^{-1}, given the I-state marker is about 70% and less than the I and P correlation (i.e. 88%). A considerable presence of I and trans Raman marker (1280 cm^{-1}) correlation, about 39%, implies that "Förster cycle" might also occur between I and C-states of the GFP chromophore.

4. This is the first report to provide evidences of observing the I-state by vibrational spectroscopy (infrared and Raman) associated with the "Förster cycle". Also the evidences are captured at single molecule level. The lack of evidences in the literature is understandable, as during the 'Förster cycle", GFP resides in the A-state for most of the part under typical fluorescence microscopy excitation conditions. As a result, limited signal can be integrated from the highly unstable I-state of the "Förster cycle". In contrast, the fraction of the time GFP chromophore resides in the I-state during the "Förster cycle" can be dramatically enhanced under the applied SM-SERS conditions. Intense optical pumping due to the surface enhancement of the nanoparticles can dramatically shorten the inhabiting time of the chromophore in the A-state. Thus, the GFP inhabits a shorter time at the ground state of A before promoting to the excited state (A*). Consequently, the inhabiting time of the I-state in the "Förster cycle" is increased and a higher signal is integrated from the I-state. Presence of metal nanoparticles in close proximity of the GFP chromophore also enhances the relaxation rate from the exited I*-state to the ground I-state. This further increases the fraction of time I-state inhabits the "Förster cycle" and facilitates the appearance of the I-state peak besides A-state or C-state in SM-SERS spectra.

5. Finally, a valid concern points towards a possible photo-degradation (i.e. photo-bleaching) of the GFP molecules under such intense surface enhanced excitation. But this concern is mitigated as the fluorescence of the GFP chromophore is effectively quenched due to the presence of the metal nanoparticles. Thus GFP chromophore can undergo an efficient excitation and deexcitation cycle (i.e. "Förster cycle") before eventual photo-degradation and loss of dynamics. This quenching of fluorescence is also beneficial towards acquiring vibrational spectra. Broad background emanating from the fluorescence is eliminated effectively and the chromophore vibrational modes can now be clearly resolved by Raman peaks at single molecule level.

These unique results are pivotal to construct a framework for future investigations confirming the effective detection and modulation of chromophore states in the "Förster cycle". An extensive quantum mechanical modeling of the "Förster cycle" can also be investigated. But, SM-SERS is proved to be a particularly efficient tool to probe and understand such dynamic photo-cycles with high structural sensitivity. These results can certainly structure and devise intelligent methods to get deeper insight on utilizing the promising photo-cycle (i.e. Förster cycle) of this Nobel Prize winning protein for photo-modulation.

REFERENCES

1.   Tsien, R.Y., *THE GREEN FLUORESCENT PROTEIN.* Annual Review of Biochemistry, 1998. **67**(1): p. 509-544.

2.   Meech, S.R., *Excited state reactions in fluorescent proteins.* Chemical Society Reviews, 2009. **38**(10): p. 2922-2934.

3.   Livet, J., et al., *Transgenic strategies for combinatorial expression of fluorescent proteins in the nervous system.* Nature, 2007. **450**(7166): p. 56-+.

4.   Gather, M.C. and S.H. Yun, *Single-cell biological lasers.* Nat Photon, 2011. **5**(7): p. 406-410.

5.   Ormö, M., et al., *Crystal Structure of the Aequorea victoria Green Fluorescent Protein.* Science, 1996. **273**(5280): p. 1392-1395.

6.   Yang, F., L.G. Moss, and G.N. Phillips, *The molecular structure of green fluorescent protein.* Nature Biotechnology, 1996. **14**(10): p. 1246-1251.

7.   Brejc, K., et al., *Structural basis for dual excitation and photoisomerization of the Aequorea victoria green   fluorescent   protein.* Proceedings of the National Academy of Sciences, 1997. **94**(6): p. 2306-2311.

8.   Maddalo, S.L. and M. Zimmer, *The Role of the Protein Matrix in Green Fluorescent Protein Fluorescence.* Photochemistry and Photobiology, 2006. **82**(2): p. 367-372.

9.   Youvan, D.C. and M.E. Michel-Beyerle, *Structure and fluorescence mechanism of GFP.* Nat Biotech, 1996. **14**(10): p. 1219-1220.

10.   Chattoraj, M., et al., *Ultra-fast excited state dynamics in green fluorescent protein: multiple states and proton transfer.* Proceedings of the National Academy of Sciences, 1996. **93**(16): p. 8362-8367.

.

11.   Striker, G., et al., *Photochromicity and fluorescence lifetimes of green fluorescent protein.* Journal of Physical Chemistry B, 1999. **103**(40): p. 8612-8617.

12.   Creemers, T.M.H., et al., *Three photoconvertible forms of green fluorescent protein identified by spectral hole-burning.* Nat Struct Mol Biol, 1999. **6**(6): p. 557-560.

13.   van Thor, J.J., et al., *Phototransformation of green fluorescent protein with UV and visible light leads to decarboxylation of glutamate 222.* Nature Structural Biology, 2002. **9**(1): p. 37-41.

14.   van Thor, J.J., et al., *Structural events in the photocycle of green fluorescent protein.* Journal of Physical Chemistry B, 2005. **109**(33): p. 16099-16108.

15.   Schellenberg, P., et al., *Resonance Raman scattering by the green fluorescent protein and an analogue of its chromophore.* Journal of Physical Chemistry B, 2001. **105**(22): p. 5316-5322.

16.   He, X., A.F. Bell, and P.J. Tonge, *Isotopic labeling and normal-mode analysis of a model green fluorescent protein chromophore.* Journal of Physical Chemistry B, 2002. **106**(23): p. 6056-6066.

17.   Bell, A.F., et al., *Probing the ground state structure of the green fluorescent protein chromophore using Raman spectroscopy.* Biochemistry, 2000. **39**(15): p. 4423-4431.

18.   Stoner-Ma, D., et al., *Observation of Excited-State Proton Transfer in Green Fluorescent Protein using Ultrafast Vibrational Spectroscopy.* Journal of the American Chemical Society, 2005. **127**(9): p. 2864-2865.

19.   Esposito, A.P., et al., *Vibrational spectroscopy and mode assignments for an analog of the green fluorescent protein chromophore.* Journal of Molecular Structure, 2001. **569**(1-3): p. 25-41.

20.   Habuchi, S., et al., *Single-Molecule Surface Enhanced Resonance Raman Spectroscopy of the Enhanced Green Fluorescent Protein.* Journal of the American Chemical Society, 2003. **125**(28): p. 8446-8447.

21.   Kalkan, A.K. and S.J. Fonash, *Electroless Synthesis of Ag Nanoparticles on Deposited Nanostructured Si Films.* The Journal of Physical Chemistry B, 2005. **109**(44): p. 20779-20785.

22.   Kalkan, A.K. and S.J. Fonash, *Laser-activated surface-enhanced Raman scattering substrates capable of single molecule detection.* Applied Physics Letters, 2006. **89**(23): p. 233103-3.

23.   Fang, C., et al., *Mapping GFP structure evolution during proton transfer with femtosecond Raman spectroscopy.* Nature, 2009. **462**(7270): p. 200-U74.

24.   Singhal, K. and A.K. Kalkan, *Surface-Enhanced Raman Scattering Captures Conformational Changes of Single Photoactive Yellow Protein Molecules under Photoexcitation.* Journal of the American Chemical Society, 2009. **132**(2): p. 429-431.

25.   Campion, A. and P. Kambhampati, *Surface-enhanced Raman scattering.* Chemical Society Reviews, 1998. **27**(4): p. 241-250.

26.   Otto, A. and et al., *Surface-enhanced Raman scattering.* Journal of Physics: Condensed Matter, 1992. **4**(5): p. 1143.

27.   Haynes, C.L., A.D. McFarland, and R.P. Van Duyne, *Surface-enhanced Raman spectroscopy.* Analytical Chemistry, 2005. **77**(17): p. 338a-346a.

28.   Nie, S. and S.R. Emory, *Probing Single Molecules and Single Nanoparticles by Surface-Enhanced Raman Scattering.* Science, 1997. **275**(5303): p. 1102-1106.

29.   Moerner, W.E., *A dozen years of single-molecule spectroscopy in physics, chemistry, and biophysics.* Journal of Physical Chemistry B, 2002. **106**(5): p. 910-927.

30.   Le Ru, E.C., M. Meyer, and P.G. Etchegoin, *Proof of Single-Molecule Sensitivity in Surface Enhanced Raman Scattering (SERS) by Means of a Two-Analyte Technique.* The Journal of Physical Chemistry B, 2006. **110**(4): p. 1944-1948.

31.   Etchegoin, P.G. and E.C. Le Ru, *Resolving Single Molecules in Surface-Enhanced Raman Scattering within the Inhomogeneous Broadening of Raman Peaks.* Analytical Chemistry, 2010. **82**(7): p. 2888-2892.

32.   Shimomura, O., F.H. Johnson, and Y. Saiga, *Extraction, Purification and Properties of Aequorin, a Bioluminescent Protein from Luminous Hydromedusan, Aequorea.* Journal of Cellular and Comparative Physiology, 1962. **59**(3): p. 223-&.

33.   Davenport, D. and J.A.C. Nicol, *Luminescence in Hydromedusae.* Proceedings of the Royal Society of London Series B-Biological Sciences, 1955. **144**(916): p. 399-411.

34.   Shimomur.O, F.H. Johnson, and H. Morise, *Mechanism of Luminescent Intramolecular Reaction of Aequorin.* Biochemistry, 1974. **13**(16): p. 3278-3286.

35.   Shimomura, O. and F.H. Johnson, *Peroxidized Coelenterazine, Active Group in Photoprotein Aequorin.* Proceedings of the National Academy of Sciences of the United States of America, 1978. **75**(6): p. 2611-2615.

36.   Head, J.F., et al., *The crystal structure of the photoprotein aequorin at 2.3 angstrom resolution.* Nature, 2000. **405**(6784): p. 372-376.

37.   Shimomura, O., *The discovery of aequorin and green fluorescent protein.* Journal of Microscopy-Oxford, 2005. **217**: p. 3-15.

38.   Morise, H., et al., *Intermolecular Energy-Transfer in Bioluminescent System of Aequorea.* Biochemistry, 1974. **13**(12): p. 2656-2662.

39.   Perozzo, M.A., et al., *X-Ray-Diffraction and Time-Resolved Fluorescence Analyses of Aequorea Green Fluorescent Protein Crystals.* Journal of Biological Chemistry, 1988. **263**(16): p. 7713-7716.

40.   Prasher, D.C., et al., *Primary Structure of the Aequorea-Victoria Green-Fluorescent Protein.* Gene, 1992. **111**(2): p. 229-233.

41.   Cody, C.W., et al., *Chemical-Structure of the Hexapeptide Chromophore of the Aequorea Green-Fluorescent Protein.* Biochemistry, 1993. **32**(5): p. 1212-1218.

42.   Zimmer, M., *Green fluorescent protein (GFP): Applications, structure, and related photophysical behavior.* Chemical Reviews, 2002. **102**(3): p. 759-781.

43.   Ward, W.W. and S.H. Bokman, *Reversible Denaturation of Aequorea Green-Fluorescent Protein - Physical Separation and Characterization of the Renatured Protein.* Biochemistry, 1982. **21**(19): p. 4535-4540.

44.   Bokman, S.H. and W.W. Ward, *Renaturation of Aequorea Green-Fluorescent Protein.* Biochemical and Biophysical Research Communications, 1981. **101**(4): p. 1372-1380.

45.   Chen, M.C., et al., *Photoisomerization of green fluorescent protein and the dimensions of the chromophore cavity.* Chemical Physics, 2001. **270**(1): p. 157-164.

46.   Voliani, V., et al., *Cis-trans photoisomerization of fluorescent-protein chromophores.* Journal of Physical Chemistry B, 2008. **112**(34): p. 10714-10722.

47.   Nifosì, R. and V. Tozzini, *Cis-trans photoisomerization of the chromophore in the green fluorescent protein variant E2GFP: A molecular dynamics study.* Chemical Physics, 2006. **323**(2-3): p. 358-368.

48.   Bell, A.F., et al., *Light-Driven Decarboxylation of Wild-Type Green Fluorescent Protein†.* Journal of the American Chemical Society, 2003. **125**(23): p. 6919-6926.

49.   Heim, R., D.C. Prasher, and R.Y. Tsien, *Wavelength Mutations and Posttranslational Autoxidation of Green Fluorescent Protein.* Proceedings of the National Academy of Sciences of the United States of America, 1994. **91**(26): p. 12501-12504.

50.   Craggs, T.D., *Green fluorescent protein: structure, folding and chromophore maturation.* Chemical Society Reviews, 2009. **38**(10): p. 2865-2875.

51.   van Thor, J.J., et al., *Balance between ultrafast parallel reactions in the green fluorescent protein has a structural origin.* Biophysical Journal, 2008. **95**(4): p. 1902-1912.

52.   Seward, H.E. and C.R. Bagshaw, *The photochemistry of fluorescent proteins: implications for their biological applications.* Chemical Society Reviews, 2009. **38**(10): p. 2842-2851.

53.   van Thor, J.J., *Photoreactions and dynamics of the green fluorescent protein.* Chemical Society Reviews, 2009. **38**(10): p. 2935-2950.

54.   Agmon, N., *Elementary steps in excited-state proton transfer.* Journal of Physical Chemistry A, 2005. **109**(1): p. 13-35.

55.	Leiderman, P., D. Huppert, and N. Agmon, *Transition in the temperature-dependence of GFP fluorescence: From proton wires to proton exit.* Biophysical Journal, 2006. **90**(3): p. 1009-1018.

56.	Lemay, N.P., et al., *The role of the tight-turn, broken hydrogen bonding, Glu222 and Arg96 in the post-translational green fluorescent protein chromophore formation.* Chemical Physics, 2008. **348**(1-3): p. 152-160.

57.	Lossau, H., et al., *Time-resolved spectroscopy of wild-type and mutant Green Fluorescent Proteins reveals excited state deprotonation consistent with fluorophore-protein interactions.* Chemical Physics, 1996. **213**(1-3): p. 1-16.

58.	Raman, C.V., *The Raman effect. Investigation of molecular structure by light scattering.* Transactions of the Faraday Society, 1929. **25**: p. 0781-0791.

59.	Raman, C.V. and K.S. Krishnan, *A new type of secondary radiation.* Nature, 1928. **121**: p. 501-502.

60.	Smekal, A., *Zur Quantentheorie der Dispersion.* Naturwissenschaften, 1923. **11**(43): p. 873-875.

61.	Dent, E.S.a.G., *Modern Raman spectroscopy – a practical approach.* 2004: John Wiley and Sons.

62.	Gardiner, D.J., *Practical Raman Spectroscopy.* 1989: Springer.

63.	Kneipp, K., et al., *Single molecule detection using surface-enhanced Raman scattering (SERS).* Physical Review Letters, 1997. **78**(9): p. 1667-1670.

64.	Kneipp, K., et al., *Approach to Single-Molecule Detection Using Surface-Enhanced Resonance Raman-Scattering (Serrs) - a Study Using Rhodamine 6g on Colloidal Silver.* Applied Spectroscopy, 1995. **49**(6): p. 780-784.

65.	Fleischm.M, P.J. Hendra, and Mcquilla.Aj, *Raman-Spectra of Pyridine Adsorbed at a Silver Electrode.* Chemical Physics Letters, 1974. **26**(2): p. 163-166.

66.	Jeanmaire, D.L. and R.P. Van Duyne, *Surface raman spectroelectrochemistry: Part I. Heterocyclic, aromatic, and aliphatic amines adsorbed on the anodized silver electrode.* Journal of Electroanalytical Chemistry and Interfacial Electrochemistry, 1977. **84**(1): p. 1-20.

67.	Albrecht, M.G. and J.A. Creighton, *Anomalously intense Raman spectra of pyridine at a silver electrode.* Journal of the American Chemical Society, 1977. **99**(15): p. 5215-5217.

68.	Etchegoin, P.G. and E.C. Le Ru, *A perspective on single molecule SERS: current status and future challenges.* Physical Chemistry Chemical Physics, 2008. **10**(40): p. 6079-6089.

69.	Otto, A., *What is observed in single molecule SERS, and why?* Journal of Raman Spectroscopy, 2002. **33**(8): p. 593-598.

70.   Xu, H.X., et al., *Spectroscopy of single hemoglobin molecules by surface enhanced Raman scattering.* Physical Review Letters, 1999. **83**(21): p. 4357-4360.

71.   Moskovits, M., *Surface-enhanced spectroscopy.* Reviews of Modern Physics, 1985. **57**(3): p. 783.

72.   Moskovits, M., *Surface-Enhanced Raman Spectroscopy: a Brief Perspective*, in *Surface-Enhanced Raman Scattering*, K. Kneipp, M. Moskovits, and H. Kneipp, Editors. 2006, Springer Berlin / Heidelberg. p. 1-17.

73.   Haran, G., *Single-Molecule Raman Spectroscopy: A Probe of Surface Dynamics and Plasmonic Fields.* Accounts of Chemical Research, 2010. **43**(8): p. 1135-1143.

74.   Xu, H., et al., *Electromagnetic contributions to single-molecule sensitivity in surface-enhanced Raman scattering.* Physical Review E, 2000. **62**(3): p. 4318.

75.   Lombardi, J.R. and R.L. Birke, *A unified approach to surface-enhanced Raman spectroscopy.* Journal of Physical Chemistry C, 2008. **112**(14): p. 5605-5617.

76.   Haran, G., *Single molecule raman spectroscopy and local work function fluctuations.* Israel Journal of Chemistry, 2004. **44**(4): p. 385-390.

77.   Lee, P.C. and D. Meisel, *Adsorption and Surface-Enhanced Raman of Dyes on Silver and Gold Sols.* Journal of Physical Chemistry, 1982. **86**(17): p. 3391-3395.

78.   Khurshid, M.S., *Conformational states and transitions in green fluorescent protein chromophore studied by single molecule SERS* in *Mechanical and Aerospace Engineering*. 2011, Oklahoma State University: Stillwater.

79.   Eric Le Ru , P.E., *Principles of Surface-Enhanced Raman Spectroscopy: and related plasmonic effects*. 2008: Elsevier Science.

80.   Loos, D.C., et al., *Photoconversion in the Red Fluorescent Protein from the Sea Anemone Entacmaea quadricolor: Is Cis−Trans Isomerization Involved?* Journal of the American Chemical Society, 2006. **128**(19): p. 6270-6271.

81.   Weber, W., et al., *Shedding light on the dark and weakly fluorescent states of green fluorescent proteins.* Proceedings of the National Academy of Sciences, 1999. **96**(11): p. 6177-6182.

82.   Malicka, J., et al., *Effects of fluorophore-to-silver distance on the emission of cyanine-dye-labeled oligonucleotides.* Analytical Biochemistry, 2003. **315**(1): p. 57-66.

83.   Gersten, J. and A. Nitzan, *Spectroscopic Properties of Molecules Interacting with Small Dielectric Particles.* Journal of Chemical Physics, 1981. **75**(3): p. 1139-1152.

84.   Lakowicz, J.R., *Radiative decay engineering 5: metal-enhanced fluorescence and plasmon emission.* Analytical Biochemistry, 2005. **337**(2): p. 171-194.

85.	Lakowicz, J.R., et al., *Advances in surface-enhanced fluorescence.* Journal of Fluorescence, 2004. **14**(4): p. 425-441.

VITA

Natis Zad Shafiq

Candidate for the Degree of

Master of Science

Thesis: DETECTION OF FÖRSTER CYCLE IN SINGLE MOLECULES OF GREEN
FLUORESCENT PROTEIN

Major Field: Mechanical and Aerospace Engineering

Biographical:
Sex: Male
DOB: 02/19/1984
Hometown: Dhaka, Bangladesh

Education:

Completed the requirements for the Master of Science in Mechanical and
Aerospace Engineering at Oklahoma State University, Stillwater, Oklahoma in
July, 2011.

Completed the requirements for the Bachelor of Science in Mechanical
Engineering at Bangladesh University of Engineering and Technology, Dhaka,
Bangladesh in 2007.

Experience:
Graduate Research Assistant, MAE, OSU Stillwater (Aug 2008- July 2011)
Graduate Teaching Assistant, MAE, OSU Stillwater (Aug 2008-May 2010)

Professional Memberships:
Student Member, Materials Research Society (MRS)

Name: Natis Zad Shafiq   Date of Degree: July, 2011

Institution: Oklahoma State University   Location: Stillwater, Oklahoma

Title of Study: DETECTION OF FÖRSTER CYCLE IN SINGLE MOLECULES OF
                 GREEN FLUORESCENT PROTEIN

Pages in Study: 73   Candidate for the Degree of Master of Science

Major Field: Mechanical and Aerospace Engineering

Green Fluorescent Protein (GFP) from the jellyfish *Aequorea Victoria* earned a Nobel Prize in 2008 for being an exceptionally exploitable biological marker in the living systems. The dominant absorption band at 395 nm of GFP consists of a protonated form (A) of the chromophore and involves a protolytic reaction that forms an excited anion of the intermediate form (I^*) from the photo-excited protonated form (A^*), which upon fast relaxation to the intermediate (I) ground state repopulates the protonated (A) form. The present work reports the observation of this proton movement cycle in the excited state of GFP (i.e. $A \rightarrow A^* \rightarrow I^* \rightarrow I \rightarrow A$, Förster cycle) by acquiring vibrational spectra of single GFP molecule using "nanometal-on-semiconductor" SERS substrates and applying a "pump and probe" technique. A new peak at 1510 cm^{-1} prominently exists with the protonated form (1560 cm^{-1}). Statistical analysis of the GFP population reveals a higher probability (about 9 times) of observing both 1510 cm^{-1} and 1560 cm^{-1} peak over the probability of finding both 1510 cm^{-1} and 1530 cm^{-1} in one 'spectral jump'. We recognize this unique Raman peak at 1510 cm^{-1} as a marker for the intermediate form of the chromophore. This peak is also observed both in 'Cis' and 'Trans' configuration of the chromophore, but considerably more with 'Cis' configuration.

ADVISER'S APPROVAL: Dr. Ali Kaan Kalkan